10

Communications

Nonlinear optics is the branch of optics that describes the behavior of light in nonlinear media; such as, media in which the induced dielectric polarization responds nonlinearly to the electric field of the light. This nonlinearity is typically observed at very high light intensities such as those provided by pulsed lasers. In this chapter, we focus on the application of high bit-rate communications. We will see that the nonlinear Schrödinger (NLS) equation and the dispersion-managed nonlinear Schrödinger (DMNLS) equation play a central role.

10.1 Communications

In 1973 Hasegawa and Tappert (Hasegawa and Tappert, 1973a; Hasegawa and Kodama, 1995) showed that the nonlinear Schrödinger equation derived in Chapter 7 [see (7.26), and the subsequent discussion] described the propagation of quasi-monochromatic pulses in optical fibers. Motivated by the fact that the NLS equation supports special stable, localized, soliton solutions, Mollenauer et al. (1980) demonstrated experimentally that solitons can propagate in a real fiber. However, it was soon apparent that due to unavoidable damping in optical fibers, solitons lose most of their energy over relatively short distances. In the mid-1980s all-optical amplifiers (called erbium doped fiber amplifiers: EDFAs) were developed. However with such amplifiers there is always some additional small amount of noise. Gordon and Haus (1986) (see also Elgin, 1985) showed that solitons suffered seriously from these noise effects. The frequency and temporal position of the soliton was significantly shifted over long distances, thereby limiting the available transmission distance and speed of soliton-based systems. Subsequently researchers began to seriously consider so-called wavelength division multiplexed (WDM)

communication systems in which many optical pulses are transmitted simultaneously. The inevitable pulse interactions caused other serious problems, called four-wave mixing instabilities and collision-induced time shifts. In order to alleviate these penalties, researchers began to study dispersion-managed (DM) transmission systems. A DM transmission line consists of fibers with different types of dispersion fused together. The success of DM technology has already led to its use in commercial systems. In this chapter we discuss some of the important issues in the context of nonlinear waves and asymptotic analysis. There are a number of texts that cover this topic, which the interested reader can consult. These include Agrawal (2002, 2001), Hasegawa and Kodama (1995), Hasegawa and Matsumoto (2002), and Molleneauer and Gordon (2006).

10.1.1 The normalized NLS equation

In Chapter 7 the NLS equation was derived for weakly nonlinear, quasi-monochromatic electromagnetic waves. It was also discussed how the NLS equation should be modified to apply to optical fibers. Using the assumption for electromagnetic fields in the x-direction

$$E_x = \varepsilon(A(Z,T)e^{i(k_3-\omega t)} + cc) + O(\varepsilon^2),$$

where $Z = \epsilon z$, $T = \epsilon t$, the NLS equation in optical fibers was found, in Chapter 7 [see (7.27) and the equations following], to satisfy

$$i\frac{\partial A}{\partial \tilde{z}} + \left(-\frac{k''(\omega)}{2}\right)\frac{\partial^2 A}{\partial T^2} + \nu|A|^2 A = 0, \tag{10.1}$$

with the nonlinear coefficient $\nu = \nu_{\text{eff}} = \dfrac{n_2\omega}{4cA_{\text{eff}}}$ where the retarded coordinate frame is given by $T = \epsilon t - \dfrac{Z}{v_g} = \epsilon t - k'Z$, $\tilde{z} = \epsilon Z$ with $k = \dfrac{\omega}{c}n_0$, and the nonlinear index of refraction is given by $n = n_0 + n_2|E_x|^2 = n_0 + 4n_2|A|^2$; $v_g = 1/k'(\omega)$ is the group velocity and A_{eff} is the effective area of the fiber. It is standard to introduce the following non-dimensional coordinates: $\tilde{z} = z'z_*$, $T = t't_*$, and $A = \sqrt{P_*}u$, where a subscript $*$ denotes a characteristic scale. Usually, z_* is taken as being proportional to the nonlinear length, the length over which a nonlinear phase change of one radian occurs, t_* is taken as being proportional to the pulse full width at half-maximum (FWHM), and P_* is taken as the peak pulse power. With the use of this non-dimensionalization, (10.1) becomes

$$i\frac{\partial u}{\partial z'} + \left(\frac{z_*}{t_*^2}\right)(-k'')\frac{1}{2}\frac{\partial^2 u}{\partial t'^2} + z_* P_* \nu |u|^2 u = 0.$$

For solitons, $z_* P_* \nu = 1$ gives the nonlinear length as $z_* = 1/\nu P_*$. On the other hand the linear dispersive length is given by $z_{*L} = t_*^2/|k''|$. Further assuming the nonlinear length to be equal to the linear dispersive length, yields the relation $P_* = |k''|/\left(\nu t_*^2\right)$, and the normalized NLS equation follows:

$$i\frac{\partial u}{\partial z'} + \frac{1}{2}\frac{\partial^2 u}{\partial t'^2} + |u|^2 u = 0. \tag{10.2}$$

An exact solution of (10.2), called here the classical soliton solution, is given by $u = \eta\ \mathrm{sech}(\eta t')\, e^{i\eta^2 z'/2}$ (see also Chapter 6). As mentioned earlier, solitons in optical fibers were predicted theoretically in 1973 (Hasegawa and Tappert, 1973a) and then demonstrated experimentally a few years later (Mollenauer et al., 1980; see also Hasegawa and Kodama, 1995, for additional references and historical background).

10.1.2 FWHM: The full width at half-maximum

The FWHM corresponds to the temporal distance between the two points where the pulse is at half its peak power. This is schematically shown in Figure 10.1. For a sech pulse this gives

$$|u|^2 = \eta^2\, \mathrm{sech}^2\left(\frac{\eta T}{t_*}\right) = \frac{\eta^2}{2}.$$

Thus T is such that $\mathrm{sech}^2(\eta T/t_*) = 1/2$. If we assume $\eta = 1$, then $T/t_* \approx 1.763/2 = 0.8815$. The FWHM for classical solitons is notationally taken to be τ with $\tau = 2T \approx 1.763 t_*$. Recall that t_* is the normalizing value of

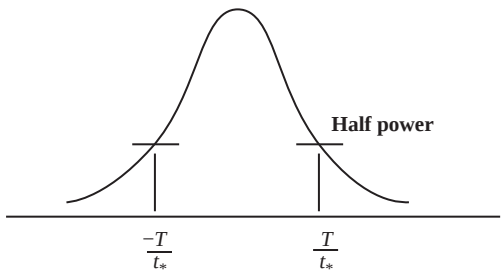

Figure 10.1 The full width at half-maximum.

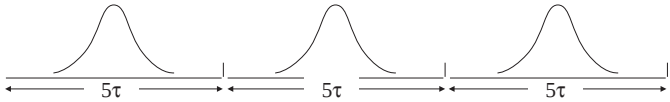

Figure 10.2 Pulses are frequently spaced five FWHM apart in a single-channel optical fiber communication system.

t. If $\tau = 20$ ps (ps denotes picoseconds) with pulse spacing of $5\tau = 100$ ps, this implies one bit is transmitted every 100 ps, as indicated in Figure 10.2. The bit-rate is therefore found to be:

$$\text{Bit-Rate} = \frac{1}{100 \times 10^{-12}} = 10 \times 10^9 \text{ bits/sec} = 10 \text{ gb/s}$$

where gb/s denotes gigabits per second. Typical numbers for classical solitons are: $\tau = 20$ ps which gives $t_* = 20/1.763 = 11.3$ ps.

On the other hand if the pulse were of Gaussian shape (which more closely approximates dispersion-managed solitons, described later in this chapter), then

$$u = u_0 e^{-t^2/2t_*^2},$$
$$|u|^2 = |u_0|^2 e^{-t^2/t_*^2} = |u_0|^2/2,$$

and

$$t = (\log 2)^{1/2} t_*,$$

hence in this case the FWHM is given by $\tau = 2\sqrt{\log\ 2}t_* = 1.665t_*$.

10.1.3 Loss

In reality there is a damping effect, or loss, in an optical fiber. Otherwise, using typical fibers, after 100 km pulses would lose most of their energy. Usually linear damping is assumed, and the NLS equation is given by

$$i\frac{\partial A}{\partial \tilde{z}} + \left(-\frac{k''(\omega)}{2}\right)\frac{\partial^2 A}{\partial T^2} + \nu|A|^2 A = -i\gamma A, \tag{10.3}$$

where γ is the physical damping rate. Non-dimensionalizing the equation as before, see (10.2), we find equation (10.3) takes the form

$$i\frac{\partial u}{\partial z} + \frac{1}{2}\frac{\partial^2 u}{\partial t^2} + |u|^2 u = -i\Gamma u, \tag{10.4}$$

where $\Gamma = \gamma z_*$ and, for convenience, we drop the prime from the variables. We can deduce the rate at which the soliton amplitude decays. Multiplying the NLS equation, (10.4), by u^* and its complex conjugate by u, we find:

$$iu^*\frac{\partial u}{\partial z} + u^*\frac{1}{2}\frac{\partial^2 u}{\partial t^2} + |u|^4 = -i\Gamma|u|^2$$
$$-iu\frac{\partial u^*}{\partial z} + u\frac{1}{2}\frac{\partial^2 u^*}{\partial t^2} + |u|^4 = i\Gamma|u|^2.$$

Noting

$$\frac{\partial(uu^*)}{\partial z} = u^*\frac{\partial u}{\partial z} + u\frac{\partial u^*}{\partial z}$$

and

$$\frac{\partial^2 u}{\partial t^2}u^* - \frac{\partial^2 u^*}{\partial t^2}u = \frac{\partial}{\partial t}\left(u^*\frac{\partial u}{\partial t} - u\frac{\partial u_*}{\partial t}\right),$$

we get, by substituting the above equations,

$$i\frac{\partial|u|^2}{\partial z}u^* + \frac{1}{2}\frac{\partial}{\partial t}\left(u^*\frac{\partial u}{\partial t} - u\frac{\partial u_*}{\partial t}\right) = -2\Gamma|u|^2,$$

and hence integrating over the (infinite) domain of the soliton pulse,

$$\frac{\partial}{\partial z}\int_{-\infty}^{\infty}|u|^2\,dt = -2\Gamma\int_{-\infty}^{\infty}|u|^2\,dt. \tag{10.5}$$

Substituting into (10.5) a classical soliton given by $u = \eta\,\mathrm{sech}(\eta t)\,e^{i\eta^2 z/2}$, we find

$$\frac{\partial}{\partial z}\int_{-\infty}^{\infty}\eta^2\,\mathrm{sech}^2(\eta t)\,dt = -2\Gamma\int_{-\infty}^{\infty}\eta^2\,\mathrm{sech}^2(\eta t)\,dt.$$

This yields the equation governing the change in the soliton parameter,

$$\frac{\partial\eta}{\partial z} = -2\Gamma\eta.$$

Thus $u = u_0 e^{-2\Gamma z}$ and we say the soliton damping rate is 2Γ. This is very different from the rate one would get if one had only a linear equation

$$i\frac{\partial u}{\partial z} + \frac{1}{2}\frac{\partial^2 u}{\partial t^2} = -i\Gamma u,$$

i.e., if we neglect the nonlinear term in (10.4). In this case, if we take $u = Ae^{i\omega t} + cc$, i.e., we assume a linear periodic wave (sometimes called "CW"

or continuous wave), we find by the same procedure as above, integrating over a period of the linear wave $T = 2\pi/\omega$:

$$\frac{\partial}{\partial z}\int_0^{\frac{2\pi}{\omega}} |A|^2\cos^2(\omega t)\,dt = -2\Gamma\int_0^{\frac{2\pi}{\omega}} |A|^2\cos^2(\omega t)\,dt$$
$$\frac{\partial}{\partial z}|A|^2 = -2\Gamma|A|^2$$
$$\frac{\partial|A|}{\partial z} = -\Gamma|A|.$$

Thus for a linear wave (CW): $|A| = |A(0)|e^{-\Gamma z}$ and therefore the amplitude of a soliton decays at "twice the linear rate"; i.e., a soliton decays at twice the damping rate as that of a linear (CW) wave.

10.1.4 Amplification

In practice, for sending signals over a long distance, in order to counteract the damping, the optical field must be amplified. A method, first developed in the mid-1980s, uses all-optical fibers (typically: "EDFAs": erbium doped fiber amplifiers)

In order to derive the relevant equation we assume the amplifiers occur at distinct locations $z_m = mz_a$, $m = 1, 2, \ldots$, down the fiber and are modeled as Dirac delta functions $(G-1)\delta(z-z_m)$, where G is the normalized gain. Here z_a denotes the normalized amplifier distance: $z_a = \ell_a/z_*$, where ℓ_a is the distance between the amplifiers in physical units. The NLS equation takes the form:

$$i\frac{\partial u}{\partial z} + \frac{1}{2}\frac{\partial^2 u}{\partial t^2} + |u|^2 u = i\left(-\Gamma + \sum_m (G-1)\delta(z-z_m)\right)u.$$

This is usually termed a "lumped" model. Integrating from $z_{n-} = z_n - \delta$ to $z_{n+} = z_n + \delta$, where $0 < \delta \ll 1$ and assuming continuity of u and its temporal derivatives

$$i\int_{z_{n-}}^{z_{n+}} \frac{\partial u}{\partial z}\,dz = i\int_{z_{n-}}^{z_{n+}} \left(-\Gamma + \sum_m (G-1)\delta(z-z_m)\right)u\,dz$$

we find

$$u(z_{n+},t) - u(z_{n-},t) = (G-1)u(z_{n-},t)$$
$$u(z_{n+},t) = Gu(z_{n-},t).$$

This gives a jump condition between the locations just in front of and just beyond an amplifier. On the other hand, if we look inside $z_{n-1+} < z < z_{n-}$ and assume $u = A(z)\tilde{u}$ inside $z_{n-1+} < z < z_{n-}$, we have

$$iA_z\tilde{u} + iA\frac{\partial\tilde{u}}{\partial z} + \frac{1}{2}A\frac{\partial^2\tilde{u}}{\partial t^2} + |A|^2A|\tilde{u}|^2\tilde{u} = i\left[-\Gamma + (G-1)\delta(z-z_{n-})\right]A\tilde{u}.$$

We take $A(z)$ to satisfy

$$\frac{\partial A}{\partial z} = \left[-\Gamma + (G-1)\delta(z-z_{n-})\right]A. \tag{10.6}$$

If we assume

$$A(z) = A_0e^{-\Gamma(z-z_{n-1})}, \quad z_{n-1+} < z < z_{n-} \tag{10.7}$$

then $A(z_{n-}) = A_0e^{-\Gamma z_a}$ and then integration of (10.6) using (10.7) yields,

$$A(z_{n+}) - A(z_{n-}) = (G-1)A(z_{n-}),$$

which implies $A(z_{n+}) = GA(z_{n-})$ consistent with the above result for u. If we further assume $A(z_{n+}) = A_0$ (i.e., A returns to its original value) then we find that the gain is $G = e^{\Gamma z_a}$ in the lumped model.

With gain-compensating loss we have the following model equation:

$$i\frac{\partial\tilde{u}}{\partial z} + \frac{1}{2}\frac{\partial^2\tilde{u}}{\partial t^2} + |A(z)|^2\,|\tilde{u}|^2\,\tilde{u} = 0,$$

where $A(z)$ is a decaying exponential in $(nz_a, (n+1)z_a)$ given by $|A|^2 = |A_0|^2e^{-2\Gamma(z-nz_a)}$, $nz_a < z < (n+1)z_a$, periodically extended (see Figure 10.3).

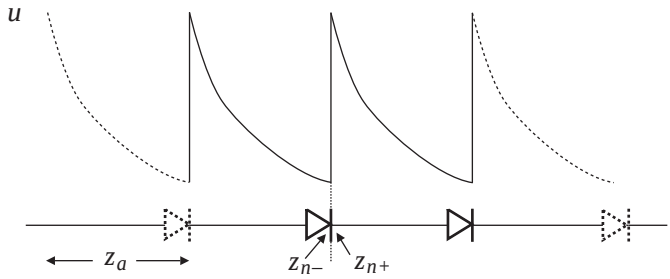

Figure 10.3 The loss of energy of the soliton u and periodic amplification.

In this model $\tilde{u}$ (unlike u) does not have delta functions in the equation and does not change discontinuously over one period. We choose $|A|^2$ such that $\frac{1}{z_a}\int_0^{z_a} |A|^2\, dz = 1$; hence

$$\frac{1}{z_a}|A_0|^2 \int_0^{z_a} e^{-2\Gamma z} dz = \frac{|A_0|^2}{-2\Gamma z_a}(e^{-2\Gamma z_a} - 1) = 1,$$

$$|A_0|^2 = \frac{2\Gamma z_a}{1 - e^{2\Gamma z_a}}.$$

Note that as $z_a \to 0$ we have $\frac{2\Gamma z_a}{1 - e^{2\Gamma z_a}} \to 1$.

For notational convenience, we now drop the tilde on u – but stress that the "true" normalized field is $u = A(z)\tilde{u}$, with $A = A_0 e^{-\Gamma(z - z_n)}$ where $nz_a < z < (n+1)z_a$ periodically extended. Thus, in summary, our basic gain/loss model is the "distributed" equation

$$i\frac{\partial u}{\partial z} + \frac{1}{2}\frac{\partial^2 u}{\partial t^2} + g(z)|u|^2 u = 0, \tag{10.8}$$

where $g(z) = |A_0|^2 e^{-2\Gamma(z - nz_a)}$, $nz_a < z < (n+1)z_a$, periodically extended. Note again that amplification occurs between $z_{n-} < z < z_{n+}$. We also see that the average of g is given by $\langle g \rangle = \frac{1}{za}\int_0^{z_a} g(z) dz = 1$. This is important regarding multi-scale theory; on average we will see that we get the unperturbed NLS equation, $iu_z + \frac{1}{2}u_{tt} + |u|^2 u = 0$.

10.1.5 Some typical units: Classical solitons

Below we list some typical classical soliton parameter values and useful relationships, where $k = 2\pi/\lambda$ and $\omega/k = c$ (here, as is standard, k is wave number, ω is frequency etc.):

$$\lambda \sim 1550\,\text{nm}; \qquad c = 3 \times 10^8\,\text{m/s}; \qquad D \sim 0.5\,\frac{\text{ps}}{\text{nm}\cdot\text{km}};$$

$$k'' = -\frac{\lambda^2 D}{2\pi c}\frac{\text{ps}^2}{\text{km}} = -0.65\frac{\text{ps}^2}{\text{km}}; \quad \omega = 1.2 \times 10^{15}\,\text{rad/s} = 193\,\text{THz};$$

$$\tau_{\text{FWHM}} \simeq 20\,\text{ps}; \quad t_* = 11.3\,\text{ps}; \quad \nu = \frac{n_2\omega}{4cA_{\text{eff}}} \sim 2.5\frac{1}{\text{W}\cdot\text{km}}; \quad P_* \sim 2\,\text{mW};$$

$$z_* \sim 200\,\text{km} = \frac{1}{\nu P_*} = \frac{1}{(2.5)(2\times 10^{-3})} = \frac{1}{5} \times 10^3 = 200\,\text{km};$$

$$z_a \sim \frac{20\,\text{km}}{200\,\text{km}} \sim 0.1; \quad \gamma = 0.05\,\frac{1}{km};$$

$$\gamma_{\text{decibels}} = 4.343\gamma = 0.22\,\frac{\text{db}}{\text{km}}; \qquad \Gamma = \gamma z_* = 10.$$

10.2 Multiple-scale analysis of the NLS equation

We begin with (10.8),

$$i\frac{\partial u}{\partial z} + \frac{1}{2}\frac{\partial^2 u}{\partial t^2} + g(z)|u|^2 u = 0.$$

We assume that $g(z)$ is rapidly varying and denote it by $g(z) = g(z/z_a)$, where $0 < z_a \ll 1$ is the "fast" scale and $z_* \sim O(1)$ is the "slow" scale. Recall that $g(z) = A_0^2 e^{-2\Gamma(z-nz_a)}$, where $nz_a < z < (n+1)z_a$. Note that in terms of the "fast" scale z_a, this can be written

$$g(z) = A_0^2 e^{-2\Gamma z_a\left(\frac{z}{z_a}-n\right)}, \qquad n < \frac{z}{z_a} < (n+1).$$

Typically $z_a \sim 0.1$, $\Gamma = 10$ and we say that $g(z)$ is rapidly varying on a scale of length z_a. Next we assume a solution of the form $u = u(\zeta, Z, t; \epsilon)$ where $\zeta = z/z_a, Z = z$ and $\epsilon = z_a$ as our small parameter. Using

$$\frac{\partial}{\partial z} \to \frac{\partial}{\partial Z} + \frac{1}{\epsilon}\frac{\partial}{\partial \zeta},$$

we can write the NLS equation as

$$i\left(\frac{\partial u}{\partial Z} + \frac{1}{\epsilon}\frac{\partial u}{\partial \zeta}\right) + \frac{1}{2}\frac{\partial^2 u}{\partial t^2} + g(\zeta)|u|^2 u = 0.$$

Assuming the standard multiple-scale expansion

$$u = u_0 + \epsilon u_1 + \epsilon^2 u_2 + \cdots,$$

we find, to leading order, $O(1/\epsilon)$,

$$i\frac{\partial u_0}{\partial \zeta} = 0,$$

which implies u_0 is independent of the fast scale $\zeta = z/\epsilon$; we write $u_0 = U(z, t)$. At the next order, $O(1)$, we have

$$i\frac{\partial u_1}{\partial \zeta} + i\frac{\partial u_0}{\partial Z} + \frac{1}{2}\frac{\partial^2 u_0}{\partial t^2} + g(\zeta)|u_0|^2 u_0 = 0,$$

or

$$i\frac{\partial u_1}{\partial \zeta} = -\left(i\frac{\partial U}{\partial Z} + \frac{1}{2}\frac{\partial^2 U}{\partial t^2} + g(\zeta)|U|^2 U\right).$$

Therefore

$$u_1 = i\left(i\frac{\partial U}{\partial Z} + \frac{1}{2}\frac{\partial^2 U}{\partial t^2} + \langle g\rangle |U|^2 U\right)\zeta + \int_0^\zeta (g(\zeta) - \langle g\rangle)\, d\zeta\, |U|^2 U.$$

Since $g(\zeta)$ is periodic with unit period, $g(\zeta) = \langle g \rangle + \sum_{n \neq 0} g_n e^{in\zeta}$. We note that $g(\zeta) - \langle g \rangle$ has zero mean and hence is non-secular (i.e., it does not grow with ζ). The first term, however, will grow without bound, i.e., this term is secular. To remove this secular term, we take, using $\langle g \rangle = 1$,

$$i\frac{\partial U}{\partial Z} + \frac{1}{2}\frac{\partial^2 U}{\partial t^2} + |U|^2 U = 0, \tag{10.9}$$

with $u \sim U$ to first order, and we see that we regain the lossless NLS equation. This approximation is sometimes called the "guiding center" in soliton theory – see Hasegawa and Kodama (1991a,b, 1995). An alternative multiscale approach for classical solitons was employed later (Yang and Kath, 1997). Equation (10.9) was obtained at the beginning of the classical soliton era. However soon it was understood that noise limited the distance of propagation. Explicitly, for typical amplifier models, noise-induced amplitude jitter (Gordon and Haus, 1986) can reduce propagation distance (in units described earlier) from 10,000 km to about 4000–5000 km. Researchers developed tools to deal with this problem (see Yang and Kath, 1997), examples being soliton transmission control and the use of filters (see, e.g., Molleneauer and Gordon, 2006). But another serious problem was soon encountered. This is described in the following section.

10.2.1 Multichannel communications: Wavelength division multiplexing

In the mid-1990s communications systems were moving towards multichannel communications or "WDM", standing for wavelength division multiplexing. WDM allows signals to be sent simultaneously in different frequency channels. In terms of the solution of the NLS equation we assume u, for a two-channel system, to be initially composed of two soliton solutions in two different channels, $u = u_1 + u_2$ that is valid before any interaction occurs. Using classical solitons,

$$u_j = \eta_j \ \mathrm{sech}\left[\eta_j(t - \Omega_j z)\right] \ e^{i\Omega_j t + i\left(\eta^2 - \Omega_j^2\right)z/2 + i\phi_j},$$

with $\Omega_1 \neq \Omega_2$; usually we take

$$u_2 = \mathrm{sech}(t - \Omega z)\, e^{i\Omega t + i(1-\Omega^2)z/2},$$
$$u_1 = \mathrm{sech}(t + \Omega z)\, e^{-i\Omega t + i(1-\Omega^2)z/2},$$

where for simplicity $\eta_1 = \eta_2 = 1$, $\Omega_2 = -\Omega_1 = \Omega$ and we assume $\Omega \gg 1$, because in practice the different frequencies are well separated. Once interaction begins we assume a solution of the form

$$u = u_1 + u_2 + u_f, \tag{10.10}$$

where u_f is due to "four-wave mixing" and we assume $|u_f| \ll 1$ because such four-wave mixing terms generated by the interaction are small. Substituting (10.10) into (10.8) we get

$$i\frac{\partial u_1}{\partial z} + i\frac{\partial u_2}{\partial z} + i\frac{\partial u_f}{\partial z} + \frac{1}{2}\left(\frac{\partial^2 u_1}{\partial t^2} + \frac{\partial^2 u_2}{\partial t^2} + \frac{\partial^2 u_f}{\partial t^2}\right) + \\ + g(z)(u_1 + u_2 + u_f)^2(u_1^* + u_2^* + u_f^*) = 0.$$

Since $u_1, u_2 \sim O(1)$ and $|u_f| \ll 1$, we can neglect the terms containing u_f. Expanding we arrive at

$$(u_1 + u_2 + u_f)^2\left(u_1^* + u_2^* + u_f^*\right) = \\ = \underbrace{|u_1|^2 u_1 + |u_2|^2 u_2}_{\text{SPM}} + \underbrace{2|u_1|^2 u_2 + 2|u_2|^2 u_1}_{\text{XPM}} + \underbrace{u_1^2 u_2^* + u_2^2 u_1^*}_{\text{FWM}} + O(u_f),$$

where SPM means "self-phase modulation", XPM stands for "cross-phase modulation" and FWM: "four-wave mixing". Recall that the frequencies (or frequency channels) of the solitons u_j, $j = 1, 2$, are given by $u_1 \sim e^{-i\Omega t}$ and $u_2 \sim e^{i\Omega t}$, giving

$$u_1^2 u_2^* \sim e^{-3i\Omega t}$$
$$u_1^* u_2^2 \sim e^{+3i\Omega t}.$$

The equation for the above FWM components (with frequencies $\pm 3i\Omega t$) is

$$i\frac{\partial u_f}{\partial z} + \frac{1}{2}\frac{\partial^2 u_f}{\partial t^2} + g(z)\left(u_1^2 u_2^* + u_2^2 u_1^*\right) = 0. \tag{10.11}$$

On the other hand, the equation for u_1 (sometimes called channel 1), which is forced by SPM and XPM terms, is

$$i\frac{\partial u_1}{\partial z} + \frac{1}{2}\frac{\partial^2 u_1}{\partial t^2} + g(z)|u_1|^2 u_1 = -2g(z)|u_2|^2 u_1. \tag{10.12}$$

The symmetric analog for channel 2 (u_2) is

$$i\frac{\partial u_2}{\partial z} + \frac{1}{2}\frac{\partial^2 u_2}{\partial t^2} + g(z)|u_2|^2 u_2 = -2g(z)|u_1|^2 u_2. \tag{10.13}$$

Since $|\Omega_2 - \Omega_1| \gg 1$, the equations separate naturally from one another. This is most easily understood as separation of energy in Fourier space. Direct numerical simulations support this model.

10.2.2 Four-wave mixing

If we say $u_f = q + r$, where $q \sim e^{3i\Omega t}$ and $r \sim e^{-3i\Omega t}$, we can separate (10.11) into two parts:

$$iq_z + \frac{1}{2}q_{tt} + g(z)u_2^2 u_1^* = 0$$
$$ir_z + \frac{1}{2}r_{tt} + g(z)u_1^2 u_2^* = 0.$$

Let us look at the equation for q:

$$iq_z + \frac{1}{2}q_{tt} = -g(z)u_2^2 u_1^*. \tag{10.14}$$

A similar analysis can be done for r. Note that the right-hand side of (10.14) is

$$\text{RHS} = u_2^2 u_1^* = e^{+3i\Omega t - \frac{i}{2}\Omega^2 z}\,\text{sech}^2(t - \Omega z)\,\text{sech}(t + \Omega z)e^{iz/2}.$$

It is natural to assume $q = F(z,t)e^{3i\Omega t - i\Omega^2 z/2}$, where the rapidly varying phase is separated out leaving the slowly varying function $F(z,t)$. The equation for $F(z,t)$ then satisfies a linear equation

$$i\left(F_z - \frac{i}{2}\Omega^2 F\right) + \frac{1}{2}\left(F_{tt} + 6i\Omega F_t - 9\Omega^2 F\right) = -g(z)R(z,t),$$

where

$$R(z,t) = \text{sech}^2(t - \Omega z)\,\text{sech}(t + \Omega z)e^{iz/2}.$$

After simplification, $F(z,t)$ now satisfies

$$iF_z + \frac{1}{2}F_{tt} + 3i\Omega F_t - 4\Omega^2 F = -g(z)R. \tag{10.15}$$

(We remark that if we put $\omega_f = 3\Omega$ and $k_f = \dfrac{2\Omega_2^2 - \Omega_1^2}{2} = \dfrac{\Omega^2}{2}$, then the phase of $u_2^2 u_1^*$ is $e^{i(\omega_f t - k_f z)}$ and $\omega_f^2/2 - k_f = 9\Omega^2/2 - \Omega^2/2 = 4\Omega^2$.)

We may now solve (10.15) using Fourier transforms (see also Ablowitz et al., 1996). However, a simple and useful model is obtained by assuming $|F_{tt}| \ll \Omega^2 F$ and $|\Omega F_t| \ll \Omega^2 F$. In this case we have the following reduced model:

$$iF_z - 4\Omega^2 F = -g(z)R.$$

Letting $R = \tilde{R}e^{iz/2}$ leads to

$$i\frac{\partial}{\partial z}\left(Fe^{4i\Omega^2 z}\right) = -g(z)\tilde{R}e^{4i\Omega^2 z + iz/2}. \tag{10.16}$$

Near the point of collision of the solitons, i.e., at $z = 0$, there is a non-trivial contribution to F. We consider $\tilde{R}$ as constant in this reduced model. Since $g(z)$ is periodic with period z_a it can be expanded in a Fourier series, $g(z) = \sum_{-\infty}^{\infty} g_n e^{-2\pi i n z/z_a}$, in which case the right-hand side of (10.16) is proportional to

$$g(z)e^{4i\Omega^2 z + iz/2} = \sum_{-\infty}^{\infty} g_n e^{iz\left[4\Omega^2 - 2\pi n/z_a + \frac{1}{2}\right]}.$$

Then from (10.16), we see that there is an FWM *resonance* when

$$\frac{2\pi n}{z_a} = 4\Omega^2 + \frac{1}{2}, \tag{10.17}$$

where n is an integer. We therefore have the growth of FWM terms whenever (10.17) is (nearly) satisfied. Otherwise F can be expected to remain small. Thus, given Ω and z_a, the nearest integer n is given by $n = (4\Omega^2 + 1/2)z_a/2\pi$. Using the typical numbers $z_a = 0.1$, $\Omega = 4$, $n \simeq (0.1)\left(\frac{64.5}{6.28}\right) \simeq 1.03$ gives $n = 1$ as the dominant FWM contribution. See Figure 10.4 where numerical simulation of (10.1) (with typical parameters) demonstrates the significant FWM growth for classical solitons. For more information see Mamyshev and Mollenauer (1996) and Ablowitz et al. (1996).

To avoid the FWM growth/interactions (and noise effects) that created significant penalties, researchers began to use "dispersion-management" described in the following section. Dispersion-management (DM) is characterized by large varying local dispersion that changes sign. With such large local dispersion variation one expects strongly reduced FWM contribution, which has been analyzed in detail (see Ablowitz et al., 2003a).

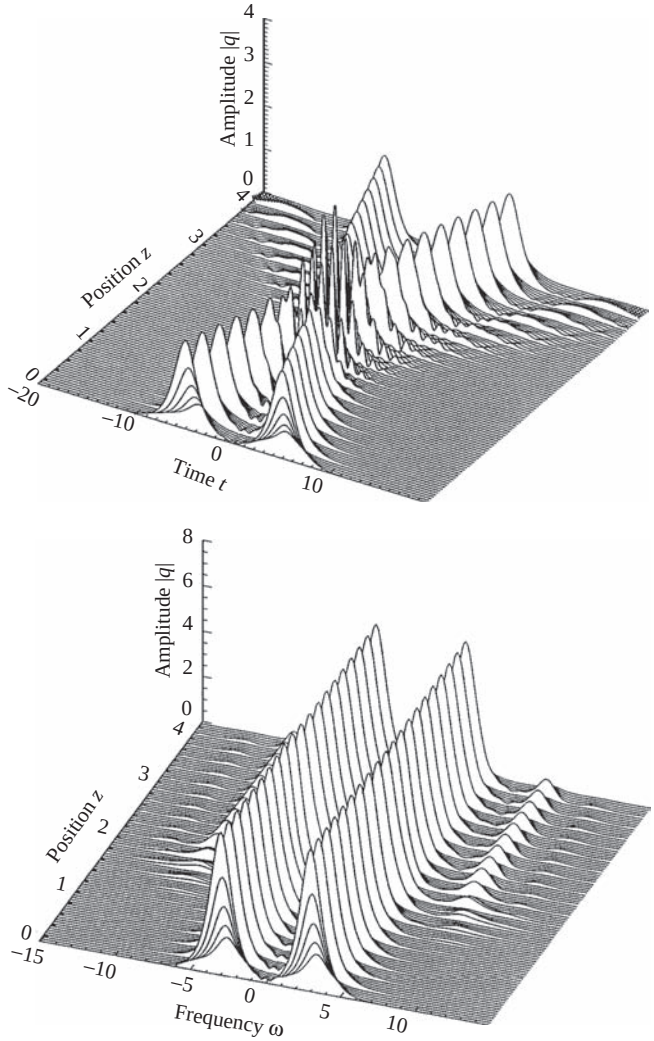

Figure 10.4 Typical two-soliton interaction. Growth of FWM components in both the physical (t) and the Fourier domain (ω) for classical solitons can be observed.

10.3 Dispersion-management

We begin with the dimensional NLS equation in the form:

$$iA_z + \frac{(-k''(z))}{2}A_{tt} + \nu|A|^2A = 0, \tag{10.18}$$

where we note that now k'' is a function of z and for simplicity we omit gain and loss for now. For classical solitons the dispersive coefficient, k'', is constant. However, with dispersion-management the dispersion varies with z and thus $k'' = k''(z)$. To normalize this equation (see also Section 10.1.1) we take $A = \sqrt{P_*}u$, $z = z_* z'$ and $t = t_* t'$; recall the nonlinear distance is given by $z_* = 1/\nu P_*$ and t_* is determined by the FWHM of the pulse, t_{FWHM}. Then (10.18) becomes

$$iu_z + \frac{(-k''(z))}{2}\frac{z_*}{t_*^2}u_{tt} + \nu P_* z_* |u|^2 u = 0.$$

Taking $k_*'' = t_*^2/z_*$ we get

$$iu_z + \frac{(-k''(z)/k_*'')}{2}u_{tt} + |u|^2 u = 0.$$

The dispersion $d(z) = -k''(z)/k_*''$ is dependent on z and can be written as an average plus a varying part, $k'' = \langle k'' \rangle + \delta k''(z)$, where $\langle k'' \rangle$ represents the average and is given by $\langle k'' \rangle = \left(k_1''\ell_1 + k_2''\ell_2\right)/\ell$ where ℓ_1 and ℓ_2 are the lengths of the anomalous and normal dispersion segments, respectively, and $\ell = \ell_1 + \ell_2$, and usually $l = l_a$ (l_a: the length between amplifiers). The non-dimensionalized dispersion is given by $k''/k_*'' = \langle d \rangle + \tilde{\Delta}(z) = d(z)$, with the average dispersion denoted by $\langle d \rangle = \langle k'' \rangle / k_*''$ and the varying part around the average: $\tilde{\Delta}(z) = \delta k''/k_*''$. Typically it is taken to be a piecewise constant function as illustrated in Figure 10.5.

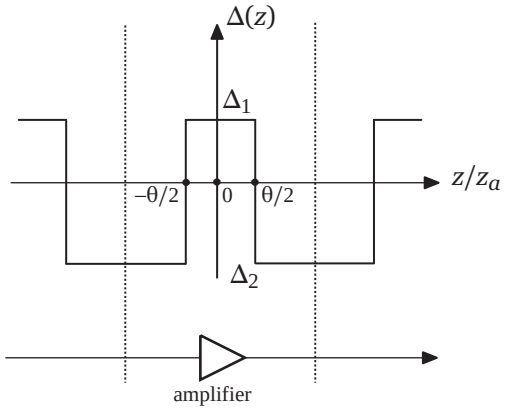

Figure 10.5 A schematic diagram of a two-fiber dispersion-managed cell. Typically the periodicity of the dispersion-management is equal to the amplifier spacing, i.e., $\ell = \ell_a$ or in normalized form, $z_a = l_a/z_*$.

The non-dimensionalized NLS equation is now

$$iu_z + \frac{d(z)}{2}u_{tt} + |u|^2 u = 0.$$

Damping and amplification can be added, as before, which leads to our fundamental model:

$$iu_z + \frac{d(z)}{2}u_{tt} + g(z)|u|^2 u = 0. \tag{10.19}$$

If $d(z)$ does not change sign, we can simplify (10.19) by letting

$$\tilde{z}(z) = \int_0^z h(z')\,dz'$$

so that $\partial_z = h(z)\partial_{\tilde{z}}$, where $h(z)$ is to be determined. Equation (10.19) then becomes

$$iu_{\tilde{z}} + \frac{1}{2}\frac{d(z)}{h(z)}u_{tt} + \frac{g(z)}{h(z)}|u|^2 u = 0.$$

If fibers could be constructed so that $h(z) = d(z) = g(z)$, then we would obtain the classical NLS equation:

$$iu_{\tilde{z}} + \frac{1}{2}u_{tt} + |u|^2 u = 0.$$

This type of fiber is called "dispersion following the loss profile".

Unfortunately, it is very difficult to manufacture such fibers. An idea first suggested in 1980 (Lin et al., 1980) that has become standard technology is to fuse together fibers that have large and different, but (nearly) constant, dispersion characteristics. A two-step "dispersion-managed" transmission line is modeled as follows:

$$d(z) = \langle d\rangle + \frac{\Delta(z/z_a)}{z_a}, \quad \langle\Delta\rangle = \int_0^1 \Delta(\zeta)\,d\zeta = 0, \quad \zeta = \frac{z}{z_a}.$$

We quantify the parameters of a two-step map as illustrated in Figure 10.5. The variation of the dispersion is given by $\Delta(\zeta)$,

$$\Delta(\zeta) = \begin{cases} \Delta_1, & 0 \le |\zeta| < \theta/2, \\ \Delta_2, & \theta/2 < |\zeta| < 1/2. \end{cases}$$

In this two-step map we usually parameterize Δ_j, $j = 1, 2$, by

$$\Delta_1 = \frac{2s}{\theta}, \qquad \Delta_2 = \frac{-2s}{1-\theta},$$

where $\langle\Delta\rangle = 0$ and s is termed the map strength parameter, defined as

$$s = \frac{\theta\Delta_1 - (1-\theta)\Delta_2}{4} = \frac{\text{area enclosed by}\Delta}{4}. \tag{10.20}$$

Note that $\langle\Delta\rangle = \theta\Delta_1 + (1-\theta)\Delta_2 = 0$, as it should be by its definition.

Remarkably dispersion-management is also an important technology that is used to produce ultra-short pulses in mode-locked lasers, such as in Ti:sapphire lasers (Ablowitz et al., 2004a; Quraishi et al., 2005; Ablowitz et al., 2008) discussed in the next chapter.

10.4 Multiple-scale analysis of DM

In this section we apply the method of multiple scales to (10.19) (see Ablowitz and Biondini, 1998):

$$iu_z + \frac{1}{2}\left(\langle d\rangle + \frac{\Delta(\zeta)}{z_a}\right)u_{tt} + g(\zeta)|u|^2u = 0. \tag{10.21}$$

In (10.21), let us call our small parameter $z_a = \varepsilon$, assume $z_a \equiv \epsilon \ll 1$, and define $u = u(t, \zeta, Z; \epsilon)$, $\zeta = z/\epsilon$, and $Z = z$; hence, $\dfrac{\partial}{\partial z} = \dfrac{1}{\epsilon}\dfrac{\partial}{\partial\zeta} + \dfrac{\partial}{\partial Z}$. Thus,

$$\frac{1}{\epsilon}\left(i\frac{\partial u}{\partial\zeta} + \frac{1}{2}\Delta(\zeta)\frac{\partial^2 u}{\partial t^2}\right) + i\frac{\partial u}{\partial Z} + \frac{1}{2}\langle d\rangle\frac{\partial^2 u}{\partial t^2} + g(\zeta)|u|^2u = 0.$$

With a standard multiple-scales expansion $u = u_0 + \epsilon u_1 + \epsilon^2 u_2 + \cdots$, we have at leading order, $O(1/\epsilon)$,

$$i\frac{\partial u_0}{\partial\zeta} + \frac{\Delta(\zeta)}{2}\frac{\partial^2 u_0}{\partial t^2} = 0. \tag{10.22}$$

We solve (10.22) using Fourier transforms, defined by (inverse transform)

$$u_0(t, \zeta, Z) \equiv \frac{1}{2\pi}\int_{-\infty}^{\infty}\hat{u}_0(\omega, \zeta, Z)e^{i\omega t}\,d\omega,$$

and (direct transform)

$$\hat{u}_0(\omega, \zeta, Z) = \mathcal{F}\{u_0\} \equiv \int_{-\infty}^{\infty}u_0(t, \zeta, Z)e^{-i\omega t}\,dt.$$

Taking the Fourier transform of (10.22) and solving the resulting ODE, we find

$$\frac{\partial \hat{u}_0}{\partial \zeta} - \frac{\omega^2}{2}\Delta(\zeta)\hat{u}_0 = 0, \tag{10.23a}$$

$$\hat{u}_0(\omega, \zeta, Z) = \hat{U}(\omega, Z)e^{-i\omega^2 C(\zeta)/2}, \tag{10.23b}$$

where $C(\zeta) = \int_0^\zeta \Delta(\zeta')\, d\zeta'$ is the integrated dispersion.

At the next order, O(1), we have

$$i\frac{\partial u_1}{\partial \zeta} + \frac{\Delta(\zeta)}{2}\frac{\partial^2 u_1}{\partial t^2} = F_1, \tag{10.24}$$

where

$$-F_1 \equiv i\frac{\partial u_0}{\partial Z} + \frac{1}{2}\langle d\rangle \frac{\partial^2 u_0}{\partial t^2} + g(\zeta)|u_0|^2 u_0.$$

Again using the Fourier transform, (10.24) becomes

$$i\hat{u}_{1\zeta} - \frac{\omega^2}{2}\Delta(\zeta)\hat{u}_1 = \widehat{F}_1,$$

or

$$i\frac{\partial}{\partial \zeta}\left(\hat{u}_1 e^{i\omega^2 C(\zeta)/2}\right) = \widehat{F}_1 e^{i\omega^2 C(\zeta)/2}.$$

Hence

$$\left[i\hat{u}_1 e^{i\omega^2 C(\zeta)/2}\right]_{\zeta'=0}^{\zeta'=\zeta} = \int_0^\zeta \widehat{F}_1 e^{i\omega^2 C(\zeta)/2}\, d\zeta.$$

Since $C(\zeta)$ is periodic in ζ and Δ has zero mean, $\hat{u}_0$ is also periodic in ζ. Therefore to remove secular terms we must have $\left\langle \widehat{F}_1 e^{i\omega^2 C(\zeta)/2}\right\rangle = 0$. Thus we require that

$$\left\langle \widehat{F}_1 e^{i\omega^2 C(\zeta)/2}\right\rangle = \int_0^1 \widehat{F}_1 e^{i\omega^2 C(\zeta)/2}\, d\zeta = 0,$$

or

$$\int_0^1 \left(i\frac{\partial \hat{u}_0}{\partial Z} - \frac{\langle d\rangle}{2}\omega^2 \hat{u}_0\right) e^{i\omega^2 C(\zeta)/2}\, d\zeta + \int_0^1 g(\zeta)\mathcal{F}\left\{|u_0|^2 u_0\right\} e^{i\omega^2 C(\zeta)/2}\, d\zeta = 0.$$

Using (10.23b) we get the dispersion-managed NLS (DMNLS) equation:

$$i\frac{\partial \hat{U}}{\partial Z} - \frac{\langle d\rangle}{2}\omega^2 \hat{U} + \left\langle g(\zeta)\mathcal{F}\left\{|u_0|^2 u_0\right\} e^{i\omega^2 C(\zeta)/2}\right\rangle = 0. \tag{10.25}$$

10.4.1 The DMNLS equation in convolution form

Equation (10.25) is useful numerically, but analytically it is often better to transform the nonlinear term to Fourier space. Using the Fourier transform

$$u_0(t,\zeta,Z) = \frac{1}{2\pi}\int_{-\infty}^{\infty} \hat{U}(\omega,Z)e^{-i\omega^2 C(\zeta)/2}e^{i\omega t}\,d\omega \tag{10.26}$$

in the nonlinear term in (10.25), we find, after interchanging integrals (see Section 10.4.2 for a detailed discussion):

$$\left\langle g(\zeta)\mathcal{F}[|u_0|^2\,u_0]e^{i\omega^2 C(\zeta)/2}\right\rangle = \int_{-\infty}^{\infty}\int_{-\infty}^{\infty} r(\omega_1\omega_2)\hat{U}(\omega+\omega_1,z) \times \hat{U}(\omega+\omega_2,z)\hat{U}^*(\omega+\omega_1+\omega_2,z)\,d\omega_1 d\omega_2, \tag{10.27}$$

where

$$r(\omega_1\omega_2) = \frac{1}{(2\pi)^2}\int_0^1 g(\zeta)\exp\left[i\omega_1\omega_2 C(\zeta)\right]\,d\zeta. \tag{10.28}$$

If $g(z) = 1$, i.e., the lossless case, we find for the two-step map, depicted in Figure 10.5, that

$$r(x) = \frac{\sin sx}{(2\pi)^2 sx}, \tag{10.29}$$

where s is called the DM map strength [see (10.20)]. This leads to another representation of the DMNLS equation in "convolution form"

$$i\hat{U}_Z - \frac{\langle d\rangle}{2}\omega^2\hat{U} + \int_{-\infty}^{\infty}\int_{-\infty}^{\infty} r(\omega_1\omega_2)\hat{U}(\omega+\omega_1,z)\hat{U}(\omega+\omega_2,z) \hat{U}^*(\omega+\omega_1+\omega_2,z)\,d\omega_1\,d\omega_2 = 0, \tag{10.30}$$

where $r(\omega_1\omega_2)$ is given in (10.28) (Ablowitz and Biondini, 1998; Gabitov and Turitsyn, 1996).

The above DMNLS equation has a natural dual in the time domain. Taking the inverse Fourier transform of (10.30) yields (see Section 10.4.2 for details)

$$iU_Z + \frac{\langle d\rangle}{2}U_{tt} + \int_{-\infty}^{\infty}\int_{-\infty}^{\infty} R(t_1,t_2)U(t_1)U(t_2)U^*(t_1+t_2-t)\,dt_1 dt_2 = 0, \tag{10.31}$$

where

$$R(t_1,t_2)=\int_{-\infty}^{\infty}\int_{-\infty}^{\infty} r(\omega_1\omega_2)e^{i\omega_1 t_2}e^{i\omega_2 t_1}\,d\omega_1\,d\omega_2.$$

Note that if $\Delta(z)\to 0$, we recover the classical NLS equation since it can be shown that as $s\to 0$, $r\to 1/(2\pi)^2$, $R(t_1,t_2)\to\delta(t_1)\delta(t_2)$, recalling that $\delta(t)=\frac{1}{2\pi}\int e^{i\omega t}\,dt$. When $g(z)=1$, the lossless case, we also find

$$R(t_1,t_2)=\frac{1}{2\pi s}\mathrm{Ci}\left(\frac{|t_1t_2|}{s}\right)$$

with

$$\mathrm{Ci}(x)=\int_x^{\infty}\frac{\cos u}{u}du.$$

10.4.2 Detailed derivation

In this subsection we provide the details underlying the derivation of (10.27) and (10.31) as well as the special cases of (10.29) when $g=1$. We start by writing (10.27) explicitly:

$$\begin{aligned}
I(\omega)=I&\equiv\left\langle g(\zeta)\mathcal{F}\left\{|u_0|^2u_0\right\}e^{i\omega^2C(\zeta)/2}\right\rangle\\
&=\int_0^1 g(\zeta)\int_{-\infty}^{\infty}dt\left[\frac{1}{2\pi}\int_{-\infty}^{\infty}\hat{U}(\omega_1,Z)e^{-i\omega_1^2C(\zeta)/2}e^{i\omega_1 t}\,d\omega_1\right]\\
&\quad\times\left[\frac{1}{2\pi}\int_{-\infty}^{\infty}\hat{U}(\omega_2,Z)e^{-i\omega_2^2C(\zeta)/2}e^{i\omega_2 t}\,d\omega_2\right]\\
&\quad\times\left[\frac{1}{2\pi}\int_{-\infty}^{\infty}\hat{U}^*(\omega_3,Z)e^{i\omega_3^2C(\zeta)/2}e^{-i\omega_3 t}\,d\omega_3\right]\\
&\quad\times e^{-i\omega t}e^{i\omega^2C(\zeta)/2}\,d\zeta.
\end{aligned}$$

Interchanging the order of integration and grouping the exponentials together,

$$\begin{aligned}
I=\int_0^1 g(\zeta)\int_{-\infty}^{\infty}\int_{-\infty}^{\infty}\int_{-\infty}^{\infty}&\left(\frac{1}{2\pi}\right)^2\hat{U}(\omega_1,Z)\hat{U}(\omega_2,Z)\\
&\times\hat{U}^*(\omega_3,Z)e^{-i\left(\omega_1^2+\omega_2^2-\omega_3^2-\omega^2\right)C(\zeta)/2}\\
&\times\frac{1}{2\pi}\int_{-\infty}^{\infty}e^{i(\omega_1+\omega_2-\omega_3-\omega)t}\,dt\,d\omega_1\,d\omega_2 d\omega_3\,d\zeta.
\end{aligned}$$

Recall that the Dirac delta function can be written as

$$\delta(\omega'-\omega)=\frac{1}{2\pi}\int_{-\infty}^{\infty}e^{i(\omega'-\omega)t}\,dt,$$

where $\omega' = \omega_1 + \omega_2 - \omega_3$. Thus, with $\omega_3 = \omega_1 + \omega_2 - \omega$,

$$I = \int_0^1 g(\zeta) \int_{-\infty}^{\infty} \int_{-\infty}^{\infty} \left(\frac{1}{2\pi}\right)^2 \hat{U}(\omega_1, Z)\hat{U}(\omega_2, Z)\hat{U}^*(\omega_1 + \omega_2 - \omega, Z) \times \exp\left[-i\left((\omega_1 + \omega_2)\omega - \omega_1\omega_2 - \omega^2\right)C(\zeta)\right] d\omega_1\, d\omega_2\, d\zeta. \quad (10.32)$$

A more symmetric form is obtained when we use

$$\left.\begin{array}{ll} \omega_1 & = \omega + \tilde{\omega}_1 \\ \omega_2 & = \omega + \tilde{\omega}_2 \end{array}\right\} \Rightarrow \omega_1 + \omega_2 - \omega = \tilde{\omega}_1 + \tilde{\omega}_2 + \omega.$$

Note that $-\omega_1\omega_2 + (\omega_1 + \omega_2)\omega = -(\omega + \tilde{\omega}_1)(\omega + \tilde{\omega}_2) + (\tilde{\omega}_1 + \tilde{\omega}_2 + \omega)\omega = -\tilde{\omega}_1\tilde{\omega}_2$. Equation (10.32) can now be written, after dropping the tildes,

$$I = \int_0^1 g(\zeta) \int_{-\infty}^{\infty} \int_{-\infty}^{\infty} \hat{U}(\omega_1 + \omega, Z)\hat{U}(\omega_2 + \omega, Z) \times \hat{U}^*(\omega_1 + \omega_2 + \omega, Z)\left(\frac{1}{2\pi}\right)^2 e^{i\omega_1\omega_2 C(\zeta)}\, d\omega_1\, d\omega_2\, d\zeta. \quad (10.33)$$

We now define the DMNLS kernel r:

$$r(x) \equiv \frac{1}{(2\pi)^2} \int_0^1 g(\zeta) e^{ixC(\zeta)}\, d\zeta.$$

Then (10.33) becomes

$$I = \int_{-\infty}^{\infty} \int_{-\infty}^{\infty} r(\omega_1\omega_2)\hat{U}(\omega_1 + \omega, Z) \times \hat{U}(\omega_2 + \omega, Z)\hat{U}^*(\omega_1 + \omega_2 + \omega, Z)\, d\omega_1\, d\omega_2,$$

which is the third term in (10.30), i.e., (10.27).

For the lossless case, i.e., $g(\zeta) = 1$ and a two-step map, $r(x)$, the analysis can be considerably simplified. We now give details of this calculation. First, for a two-step map with $C(0) = 0$

$$C(\zeta) = \int_0^{\zeta} \Delta(\zeta')\, d\zeta' = \begin{cases} \Delta_1\zeta, & 0 < \zeta < \theta/2 \\ \Delta_2\zeta + C_1, & \theta/2 < \zeta < 1 - \theta/2 \\ \Delta_1\zeta + C_2, & 1 - \theta/2 < \zeta < 1 \end{cases}$$

$$C_1 = \Delta_1\theta/2 - \Delta_2\theta/2 = (\Delta_1 - \Delta_2)\theta/2$$
$$C_2 = -\Delta_1,$$

where $C_{1,2}$ are obtained by requiring continuity at $\zeta = \theta/2, 1-\theta/2$, respectively. Recall that since $\langle\Delta\rangle = 0$, we have $\Delta_1\theta + \Delta_2(1-\theta) = 0$. Thus,

$$\begin{aligned} I &= \int_0^1 e^{ixC(\zeta)}\,d\zeta \\ &= \int_0^{\theta/2} e^{i\Delta_1\zeta x}\,d\zeta + \int_{\theta/2}^{1-\theta/2} e^{i(\Delta_2\zeta+C_1)x}\,d\zeta + \int_{1-\theta/2}^{1} e^{i(\Delta_1\zeta+C_2)x}\,d\zeta \\ I &= \frac{e^{i\Delta_1\theta x/2}-1}{i\Delta_1 x} \\ &\quad + e^{iC_1x}\left[\frac{e^{i\Delta_2(1-\theta/2)x}-e^{i\Delta_2\theta x/2}}{i\Delta_2 x}\right] + e^{iC_2x}\left[\frac{e^{i\Delta_1 x}-e^{i\Delta_1(1-\theta/2)x}}{i\Delta_1 x}\right]. \end{aligned}$$

Using $C_1 = (\Delta_1-\Delta_2)\theta/2$ and $C_2+\Delta_1 = 0$,

$$\begin{aligned} I &= \frac{e^{i\Delta_1\theta x/2}-e^{-i\Delta_1\theta/2}}{i\Delta_1 x} + \frac{e^{i(\Delta_2(1-\theta/2)x+(\Delta_1-\Delta_2)\theta/2)}-e^{i(\Delta_2\theta x/2+(\Delta_1-\Delta_2)\theta/2)}}{i\Delta_2 x} \\ I &= \frac{e^{i\Delta_1(\theta/2)x}-e^{-i\Delta_1(\theta/2)x}}{i\Delta_1 x} + \frac{e^{i\Delta_2(1-\theta)x+\Delta_1\theta/2}-e^{-i\Delta_1(\theta/2)x}}{i\Delta_2 x}. \end{aligned}$$

Then using $\Delta_2(1-\theta) = -\Delta_1\theta$, we get

$$I = \frac{e^{i\Delta_1(\theta/2)x}-e^{-i\Delta_1(\theta/2)x}}{i\Delta_1 x} - \frac{e^{i\Delta_1(\theta/2)x}-e^{-i\Delta_1(\theta/2)x}}{i\Delta_2 x}.$$

Setting $s = \dfrac{\Delta_1\theta-(1-\theta)\Delta_2}{4}$, we have $s = \dfrac{\Delta_1\theta}{2}$ and hence

$$\begin{aligned} \int_0^1 e^{iC(\zeta)x}\,d\zeta &= \frac{1}{ix}\left[I = \frac{e^{isx}-e^{-isx}}{\Delta_1} - \frac{e^{isx}-e^{-isx}}{\Delta_2}\right] \\ &= \frac{2\sin sx}{x}\left(\frac{1}{\Delta_1}-\frac{1}{\Delta_2}\right) \\ &= \frac{2\sin sx}{x}\left(\frac{1}{\Delta_1}+\frac{1-\theta}{\theta\Delta_1}\right) \\ &= \frac{2\sin sx}{\Delta_1\theta x} = \frac{\sin sx}{sx}; \end{aligned}$$

thus when $g = 1$

$$\int_0^1 e^{iC(\zeta)x}\,d\zeta = \frac{\sin sx}{sx}. \tag{10.34}$$

Next we investigate the inverse Fourier transform of (10.30). Using

$$U = \frac{1}{2\pi}\int_{-\infty}^{\infty} \hat{U}e^{i\omega t}\,d\omega$$

and taking the inverse Fourier transform of (10.30) gives

$$iU_Z + \frac{\langle d\rangle}{2}U_{tt} + \mathcal{F}^{-1}\left\langle g\mathcal{F}\left\{|u_0|^2 u_0\right\} e^{i\omega^2 C(\zeta)/2}\right\rangle = 0.$$

Now,

$$\begin{aligned}
&\mathcal{F}^{-1}\left\langle g\mathcal{F}\left\{|u_0|^2 u_0\right\} e^{i\omega^2 C(\zeta)/2}\right\rangle \\
&\quad = \int_{-\infty}^{\infty} e^{i\omega t}\left[\int_{-\infty}^{\infty}\int_{-\infty}^{\infty} r(\omega_1\omega_2)\hat{U}(\omega_1+\omega, Z)\hat{U}(\omega_2+\omega, Z)\right. \\
&\qquad \left.\times \hat{U}^*(\omega_1+\omega_2+\omega, Z)\, d\omega_1 d\omega_2\right] d\omega \\
&\quad = \int_{-\infty}^{\infty} e^{i\omega t}\int_{-\infty}^{\infty}\int_{-\infty}^{\infty} r(\omega_1\omega_2)\left[\int_{-\infty}^{\infty} U(t_1)e^{-i(\omega_1+\omega)t_1}\, dt_1\right] \\
&\qquad \times\left[\int_{-\infty}^{\infty} U(t_2)e^{-i(\omega_2+\omega)t_2}\, dt_2\right] \\
&\qquad \times\left[\int_{-\infty}^{\infty} U^*(t_3)e^{i(\omega_1+\omega_2+\omega)t_3}\, dt_3\right] d\omega_1\, d\omega_2 d\omega
\end{aligned}$$

$$\begin{aligned}
&= \int_{-\infty}^{\infty}\int_{-\infty}^{\infty} d\omega_1 d\omega_2 r(\omega_1\omega_2)\int_{-\infty}^{\infty} dt_1 U(t_1)\, dt_2 \int_{-\infty}^{\infty} U(t_2)\, dt_3 \\
&\quad \times \int_{-\infty}^{\infty} U^*(t_3)e^{i\omega_1(t_3-t_1)}e^{i\omega_2(t_3-t_2)}\underbrace{\frac{1}{2\pi}\int_{-\infty}^{\infty} e^{i\omega(t-t_1-t_2+t_3)}\, d\omega}_{\text{use } \delta(t-t_1-t_2+t_3)} \\
&= \int_{-\infty}^{\infty}\int_{-\infty}^{\infty} d\omega_1 d\omega_2 r(\omega_1\omega_2) \\
&\quad \times \int_{-\infty}^{\infty}\int_{-\infty}^{\infty} dt_1\, dt_2 U(t_1)e^{i\omega_1(t_2-t)}U(t_2)e^{i\omega_2(t_1-t)}U^*(t_1+t_2-t).
\end{aligned}$$

Thus,

$$\begin{aligned}
&\mathcal{F}^{-1}\left\langle g\mathcal{F}\left\{|u_0|^2 u_0\right\} e^{i\omega^2 C(\zeta)/2}\right\rangle \\
&\qquad = \int_{-\infty}^{\infty}\int_{-\infty}^{\infty} R(t_1, t_2)U(t_1)U(t_2)U^*(t_1+t_2-t)\, dt_1\, dt_2,
\end{aligned}$$

where

$$R(t_1, t_2) \equiv \int_{-\infty}^{\infty}\int_{-\infty}^{\infty} r(\omega_1\omega_2)e^{i\omega_1(t_2-t)}e^{i\omega_2(t_1-t)}\, d\omega_1\, d\omega_2.$$

With $t_1 = \tilde{t}_1 + t$ and $t_2 = \tilde{t}_2 + t$ (and dropping the $\sim$) we have,

$$\mathcal{F}^{-1}\left\langle g\mathcal{F}\left\{|u_0|^2 u_0\right\} e^{i\omega^2 C(\zeta)/2}\right\rangle = \int_{-\infty}^{\infty}\int_{-\infty}^{\infty} R(t_1,t_2)U(t+t_1)U(t+t_2)U^*(t+t_1+t_2)\,dt_1\,dt_2,$$

and

$$R(t_1,t_2) = \int_{-\infty}^{\infty}\int_{-\infty}^{\infty} r(\omega_1\omega_2)e^{i\omega_1 t_1 + i\omega_2 t_2}\,d\omega_1\,d\omega_2, \tag{10.35}$$

the last equality being obtained by interchanging the roles of ω_1 and ω_2, i.e., $\omega_1 \to \omega_2$ and $\omega_2 \to \omega_1$.

The expression for $R(t_1,t_2)$ can also be further simplified when $g(\zeta) = 1$. From (10.34) and (10.35),

$$R(t_1,t_2) = \frac{1}{(2\pi)^2}\int_{-\infty}^{\infty}\int_{-\infty}^{\infty} \frac{\sin s\omega_1\omega_2}{s\omega_1\omega_2} e^{i\omega_1 t_1 + i\omega_2 t_2}\,d\omega_1\,d\omega_2.$$

Letting, $\omega_1 = u_1/t_1$, $\omega_2 = u_2/t_2$

$$R(t_1,t_2) = \frac{1}{(2\pi)^2}\int_{-\infty}^{\infty}\int_{-\infty}^{\infty} \underbrace{\operatorname{sgn} t_1 \operatorname{sgn} t_2}_{\operatorname{sgn}(t_1t_2)} \frac{\sin\left(\frac{su_1u_2}{t_1t_2}\right)}{su_1u_2} e^{iu_1+iu_2}\,du_1\,du_2$$

$$= \frac{1}{(2\pi)^2 s}\int_{-\infty}^{\infty}\int_{-\infty}^{\infty} \frac{\sin\left(\frac{u_1u_2}{\gamma}\right)}{u_1u_2} e^{iu_1+iu_2}\,du_1\,du_2,$$

where $\gamma = \left|\frac{t_1t_2}{s}\right|$. Then

$$R(t_1,t_2) = \frac{1}{(2\pi)^2 s}\int_{-\infty}^{\infty}\int_{-\infty}^{\infty} \frac{\left(e^{iu_1u_2/\gamma} - e^{-iu_1u_2/\gamma}\right)}{2iu_1u_2} e^{i(u_1+u_2)}\,du_1\,du_2,$$

$$= \frac{1}{2is(2\pi)^2}\int_{-\infty}^{\infty}\int_{-\infty}^{\infty} \frac{e^{iu_1}}{u_1}\frac{\left(e^{iu_2(u_1/\gamma+1)} - e^{-iu_2(u_1/\gamma-1)}\right)}{u_2}\,du_1\,du_2.$$

Let us look at the second integral:

$$I = \int_{-\infty}^{\infty} \frac{\left(e^{iu_2(u_1/\gamma+1)} - e^{-iu_2(u_1/\gamma-1)}\right)}{u_2}\,du_2.$$

Denoting the two terms as I_1 and I_2, respectively, and using contour integration yields

$$I_1 = \oint_{-\infty}^{\infty} \frac{e^{iu_2(u_1/\gamma+1)}}{u_2}\,du_2 = +i\pi\operatorname{sgn}\left(\frac{u_1}{\gamma}+1\right)$$

$$I_2 = \oint_{-\infty}^{\infty} \frac{e^{iu_2(1-u_1/\gamma)}}{u_2}\,du_2 = +i\pi\operatorname{sgn}\left(1-\frac{u_1}{\gamma}\right),$$

where $\int_{-\infty}^{\infty}$ denotes the Cauchy principal value integral. Thus we have

$$\begin{aligned}
R(t_1,t_2) &= \frac{i\pi}{2is\,(2\pi)^2}\int_{-\infty}^{\infty}\frac{e^{iu_1}}{u_1}\left[\operatorname{sgn}\left(\frac{u_1}{\gamma}+1\right)-\operatorname{sgn}\left(1-\frac{u_1}{\gamma}\right)\right]du_1\\
&= \frac{1}{(4\pi s)\cdot 2}\left[\left(\int_{-\gamma}^{\infty}\frac{e^{iu_1}}{u_1}\,du_1-\int_{-\infty}^{-\gamma}\frac{e^{iu_1}}{u_1}\,du_1\right)\right.\\
&\quad\left.-\left(\int_{-\infty}^{\gamma}\frac{e^{iu_1}}{u_1}\,du_1-\int_{\gamma}^{\infty}\frac{e^{iu_1}}{u_1}\,du_1\right)\right]\\
&= \frac{1}{(4\pi s)\cdot 2}\left[-\int_{-\infty}^{-\gamma}\frac{e^{-iu_1}}{u_1}\,du_1-\int_{-\infty}^{-\gamma}\frac{e^{iu_1}}{u_1}\,du_1\right.\\
&\quad\left.+\int_{\gamma}^{\infty}\frac{e^{iu_1}}{u_1}\,du_1+\int_{\gamma}^{\infty}\frac{e^{-iu_1}}{u_1}\,du_1\right]\\
&= \frac{1}{4\pi s}\left[\int_{\gamma}^{\infty}\frac{\cos u_1}{u_1}\,du_1-\int_{-\infty}^{-\gamma}\frac{\cos u_1}{u_1}\,du_1\right]\\
&= \frac{1}{2\pi s}\int_{\gamma}^{\infty}\frac{\cos u_1}{u_1}\,du_1\\
&= \frac{1}{2\pi s}\int_{1}^{\infty}\frac{\cos\gamma y}{y}\,dy\equiv\frac{1}{2\pi s}C_i\left(\frac{|t_1t_2|}{s}\right).
\end{aligned}$$

where we used $\gamma=\left|\dfrac{t_1t_2}{s}\right|$.

10.4.3 Dispersion-managed solitons

DM solitons are stationary solutions of the DMNLS equation, (10.30). We now look for solutions of the form

$$\hat{U}(\omega,Z)=e^{i\lambda^2Z/2}\hat{F}(\omega),$$

where the only z-dependence is a linearly evolving phase. With this substitution, (10.30) becomes

$$\left(\frac{\lambda^2+\langle d\rangle\,\omega^2}{2}\right)\hat{F}(\omega)-\int_{-\infty}^{\infty}\int_{-\infty}^{\infty}r(\omega_1\omega_2)\hat{F}(\omega+\omega_1)\times\hat{F}(\omega+\omega_2)\hat{F}^*(\omega+\omega_1+\omega_2)\,d\omega_1\,d\omega_2=0$$

or

$$\hat{F}(\omega)=-\frac{2}{\lambda^2+\langle d\rangle\,\omega^2}\int_{-\infty}^{\infty}\int_{-\infty}^{\infty}r(\omega_1\omega_2)\hat{F}(\omega+\omega_1)\times\hat{F}(\omega+\omega_2)\hat{F}^*(\omega+\omega_1+\omega_2)\,d\omega_1\,d\omega_2. \quad (10.36)$$

Thus we wish to find fixed points of the integral equation (10.36). When $r(x)$ is not constant, obtaining closed-form solutions of this nonlinear integral equation is difficult. However we can readily obtain numerical solutions for $\langle d\rangle > 0$. Ablowitz and Biondini (1998) obtained numerical solutions using a fixed point iteration technique similar to that originally introduced by Petviashvili (1976). Below we first discuss a modification of this method called spectral renormalization, which has proven to be useful in a variety of nonlinear problems where obtaining localized solutions are of interest.

As we discussed earlier, another formulation of the non-local term is

$$\int_{-\infty}^{\infty}\int_{-\infty}^{\infty} r(\omega_1\omega_2)\hat{F}(\omega+\omega_1)\hat{F}(\omega+\omega_2)\hat{F}^*(\omega+\omega_1+\omega_2)\,d\omega_1\,d\omega_2 = \\ = \left\langle g(z)\mathcal{F}\left\{|u_0|^2\,u_0\right\} e^{i\omega^2 C(\zeta)/2} - i\lambda^2 Z/2\right\rangle$$

which is useful in the numerical schemes mentioned below. It should also be noted from the multiple-scales perturbation expansion, that u_0 is obtained by the inverse Fourier transform of

$$\hat{u}_0(\omega,\zeta,Z) = F(\omega)e^{i\lambda^2 Z/2}e^{-i\omega^2 C(\zeta)/2}.$$

The naive iteration procedure is given by

$$\hat{F}^{(m+1)}(\omega) = \frac{2}{\lambda^2+\langle d\rangle\,\omega^2}\left\langle g(z)\mathcal{F}\left\{|u_0|^2\,u_0\right\}^{(m)} e^{i\omega^2 C(\zeta)/2 - i\lambda^2 Z/2}\right\rangle \equiv \mathrm{Im}[\hat{F}], \tag{10.37}$$

where $m = 0, 1, 2, \ldots$ and $\hat{u}_0^{(m)} = \hat{F}^m(\omega)e^{-i\omega^2 C(\zeta)/2}$. At $m = 0$, $\hat{F}^{(0)}(\omega)$ is taken to be the inverse Fourier transform of a Gaussian or "sech"-type function. However, if we iterate (10.37) directly, the iteration generally diverges so we renormalize as follows.

In (10.37) we substitute $\hat{F} = \mu\hat{G}$. We then find the following iteration equations

$$\hat{G}_{n+1} = \mu_n^2 I[\hat{G}_n]$$

with

$$\mu_n^2 = \frac{(\hat{G}_n, \hat{G}_n)}{(\hat{G}_n, I[\hat{G}_n])}$$

where $(G_n, I_n) \equiv \int \hat{G}_n^*, I_n\big)\,d\omega$ and $G_0(t)$ can be a localized function, i.e., Gaussian or sech profile. In either case, the iterations converge rapidly. More details can be found in Ablowitz and Musslimani (2005) and Ablowitz and Horikis (2009a).

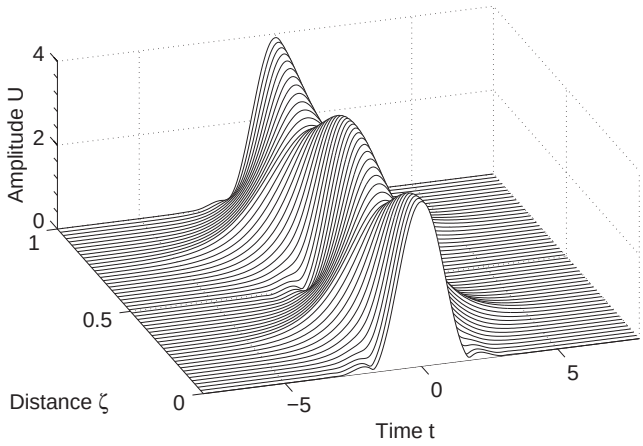

Figure 10.6 Fast evolution, $u(z,t)$, of the stationary solitons of DMNLS, reconstructed from the perturbation expansion, with $\langle d\rangle = 1$, $s = 1$ and $\lambda = 4$.

In Figure 10.6 a typical DM soliton is represented in physical space ($u \sim u^{(0)}(z,t)$). Figure 10.7 compares typical DM solitons in the Fourier and temporal domains in logarithmic scales. The dashed line is a classical soliton with the same FWHM. Figure 10.8 depicts a class of DM solitons for varying values of the map strength, s. In the figures note that $u(z,t) \sim u^{(0)}$. Hence from $\hat{u}^{(0)}(\omega) = \hat{U}(\omega, Z)e^{-iC(\zeta)\omega^2/2}$, with $\hat{U}(\omega, Z) = F(\omega)e^{i\lambda^2 Z/2}$, then $u^{(0)}(t) = \frac{1}{2\pi}\int_{-\infty}^{\infty} \hat{u}^{(0)}(\omega)e^{i\omega t}\, d\omega$. The latter yields the behavior in physical space.

Originally these methods where introduced by Petviashvili (1976) to find solutions of the KP equations. In the context of DMNLS theory (see Ablowitz et al., 2000b; Ablowitz and Musslimani, 2003) the following implementation of Petviashvili's method is employed

$$\hat{F}(\omega) = \left(\frac{S_L[\hat{F}]}{S_R[\hat{F}]}\right)^p K[\hat{F}],$$

where

$$S_L = \int_{-\infty}^{\infty} \left|\hat{F}\right|^2 \, d\omega,$$

$$S_R = \int_{-\infty}^{\infty} \hat{F}^* \cdot K[\hat{F}]\, d\omega$$

and

$$K[\hat{F}] \equiv \int_{-\infty}^{\infty}\int_{-\infty}^{\infty} r(\omega_1\omega_2)\hat{F}(\omega+\omega_1)\hat{F}(\omega+\omega_2)\hat{F}^*(\omega+\omega_1+\omega_2)\, d\omega_1 d\omega_2.$$

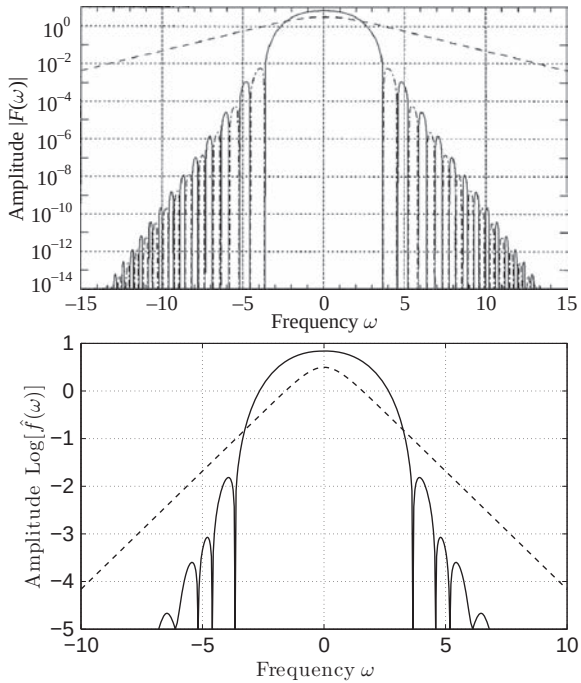

Figure 10.7 Shape of the stationary pulses in the Fourier and temporal domains for $s = 1$ and $\lambda = 4$.

The power p is usually chosen such that the degree of homogeneity of the right-hand side is zero, i.e.,

$$\deg\{\text{homog.}\}(\text{RHS}) = \frac{\hat{F}^{2p}}{\hat{F}^{4p}}\hat{F}^{3} = \hat{F}^{3-2p} \Rightarrow p = \frac{3}{2}.$$

With this choice for p, we employ the iteration scheme

$$\hat{F}^{(m+1)}(\omega) = \left(\frac{S_L[\hat{F}^{(m)}]}{S_R[\hat{F}^{(m)}]}\right)^{3/2} K[\hat{F}^{(m)}]. \tag{10.38}$$

A difficulty with this "homogeneity" method is how to handle more complex nonlinearities that do not have a fixed nonlinearity, such as mixed nonlinear terms with polynomial nonlinearity, or more complex nonlinearities, such as saturable nonlinearity $u/(1 + |u|^2)$ or transcendental nonlinearities.

We further note:

- DM solitons are well approximated by a Gaussian, $\hat{F}(\omega) \simeq ae^{-b\omega^2/2}$, for a wide range of s and λ.

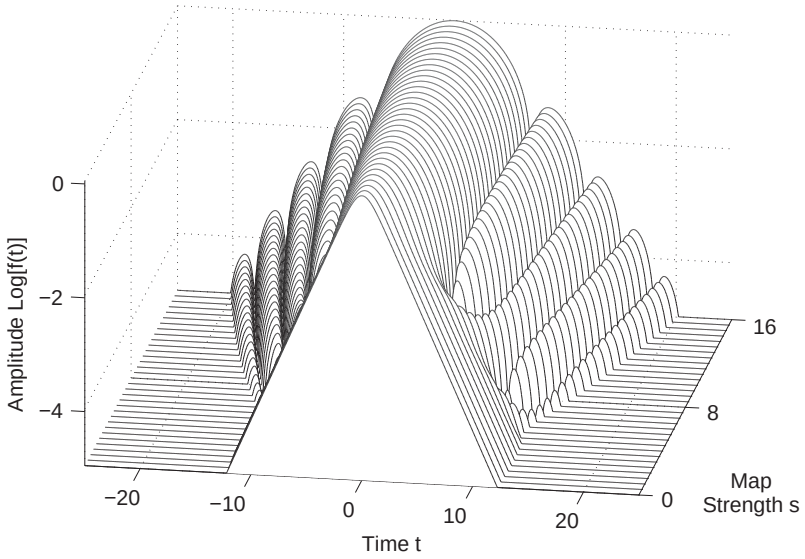

Figure 10.8 Shape of the stationary pulses in the temporal domain for $\lambda = 1$ and various values of s.

- The parameters a and b are dependent upon s and λ, $a = a(s, \lambda), b = b(s, \lambda)$.
- For $s \gg 1$, $|\hat{F}|$ grows $|\hat{F}|(\omega) \sim s^{1/2}$.

See also Lushnikov (2001).

Figure 10.9 shows "chirp" versus amplitude phase plane plots for four different DM soliton systems. This figure shows how the multi-scale approximation improves as $z_a = \varepsilon \to 0$. Here the chirp is calculated as

$$c(z) = \frac{\int_{-\infty}^{\infty} t \,\mathrm{Im}\{u^* u_t\}\, dt}{\int_{-\infty}^{\infty} t^2 |u|^2 \, dt}, \tag{10.39}$$

where $\mathrm{Im}(x)$ represents the imaginary part of x. If we approximate the DMNLS solution as a Gaussian exponential, then

$$\hat{U}_{\mathrm{DMNLS}} = a e^{-b\omega^2/2} e^{-iC(\zeta)\omega^2/2},$$

so that in the time domain, $u(t) = \dfrac{a}{\sqrt{2\pi(b + iC)}} e^{-t^2/2(b+iC)}$, then the chirp $c(z)$ is found to be given by $c(z) = C(\zeta) = C(z/z_a)$; that is also given by (10.39) after integration.

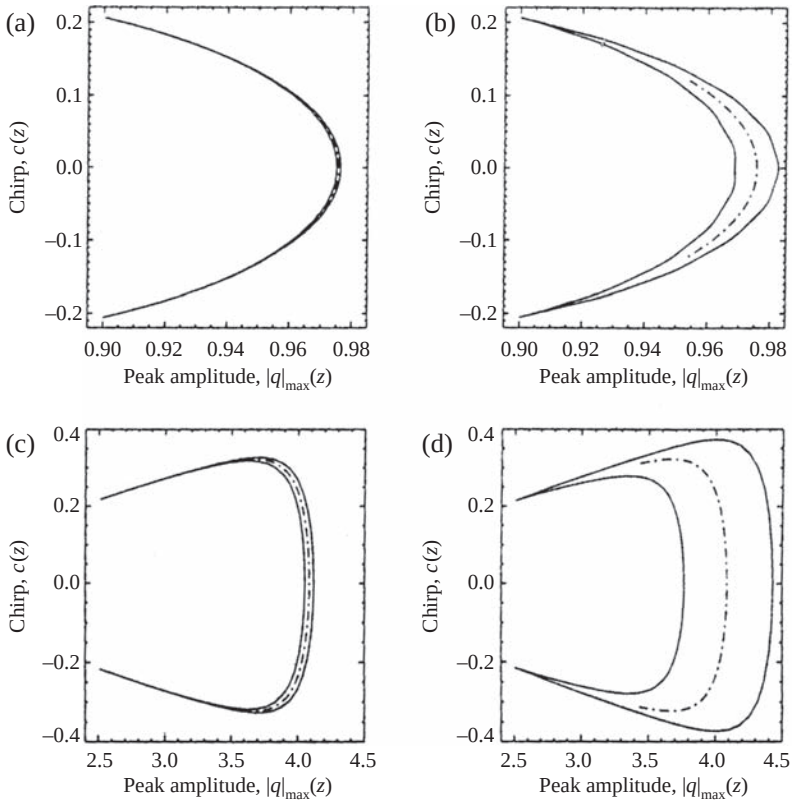

Figure 10.9 The periodic evolution of the pulse parameters: chirp $c(z)$ versus the peak amplitude. The dot–dashed line represents the leading-order approximation, $u_0(\zeta, t)$, as reconstructed from the DMNLS pulses and (10.26); the solid lines represent numerical solitions of the PNLS equation (10.19) with $g = 1$ and the same pulse energy. The four cases correspond to: (a) $s = 1$, $\lambda = 1$, $z_a = 0.02$; (b) $s = 1$, $\lambda = 1$, $z_a = 0.2$; (c) $s = 4$, $\lambda = 4$, $z_a = 0.02$; (d) $s = 4$, $\lambda = 4$, $z_a = 0.2$. The pulse energies are $\|f\|^2 = 2.27$ for cases (a) and (b), and $\|f\|^2 = 38.9$ for cases (c) and (d). See also Ablowitz et al. (2000b).

In Figure 10.10 we plot the relative L^2 norm of the difference between the stationary soliton solution of the DMNLS and the numerical solution of the original perturbed (PNLS) equation (10.19); equations with the same energy, sampled at the mid-point of the fiber segment. The difference is normalized to the L^2-norm of the numerical solution of the PNLS equation; that is

$$\frac{\|f_{\mathrm{DMNLS}} - f_{\mathrm{PNLS}}\|_2^2}{\|f_{\mathrm{PNLS}}\|} = \frac{\int_{-\infty}^{\infty} dt \ |f_{\mathrm{DMNLS}} - f_{\mathrm{PNLS}}|^2}{\int_{-\infty}^{\infty} dt \ |f_{\mathrm{PNLS}}|^2}.$$

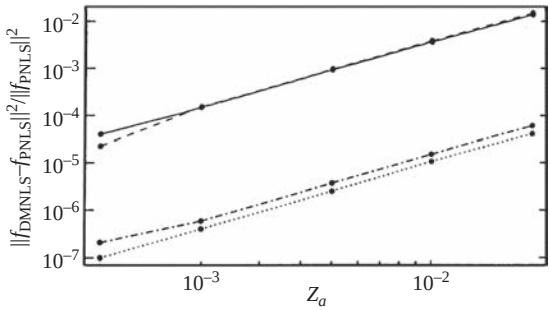

Figure 10.10 Comparison between stationary solutions of the DMNLS equation $f(t)$ and the solutions $u(z,t)$ of the PNLS equation (10.19) with the same energy taken at the mid-point of the anomalous fiber segment for $g = 1$, $\langle d\rangle = 1$ and five different values of z_a: 0.01, 0.02, 0.05, 0.1 and 0.2. Solid line: $s = 4$, $\lambda = 4$, $\|f\|^2 = 38.9$; dashed line: $s = 1$, $\lambda = 4$, $\|f\|^2 = 20.7$; dot–dashed line: $s = 4$, $\lambda = 1$, $\|f\|^2 = 3.1$; dotted line: $s = 1$, $\lambda = 1$, $\|f\|^2 = 2.27$. See also (Ablowitz et al., 2000b).

We also note there is an existence proof of DMNLS soliton solutions as ground states of a Hamiltonian. Furthermore, it can be proven that the DMNLS equation (10.30) is asymptotic, i.e., its solution remains close to the solution of the original NLS equation (10.21), see Zharnitsky et al. (2000).

10.4.4 Numerical "averaging" method

To find soliton solutions from the original PNLS equation (10.19) we may use a numerical averaging method (Nijhof et al., 1997, 2002). In this method one starts with the non-dimensional PNLS equation, (10.19):

$$iu_z + \frac{d(z)}{2}u_{tt} + g|u|^2u = 0,$$

and an initial guess for the DM soliton, e.g., a Gaussian, $u_g(z = 0, t) = u_g(t) = u^{(0)}$ with $E_0 = \int_{-\infty}^{\infty} \left|u_g\right|^2 dt$. Next, numerically integrate from $z = 0$ to $z = z_a$ to get $u(z = z_a, t)$; call this $\tilde{u}(t) = |u(t)|\, e^{i\theta(t)}$. Then one takes the following "average":

$$\tilde{\tilde{u}}(t) = \frac{u_g(t) + \tilde{u}(t)e^{-i\theta(0)}}{2}.$$

Then $u^{(1)}$ is obtained by renormalizing the energy: $u^{(1)} = \tilde{\tilde{u}}(t)\sqrt{\dfrac{E_0}{\tilde{\tilde{E}}}}$, where $\tilde{\tilde{E}} = \int_{-\infty}^{\infty} \left|\tilde{\tilde{u}}^2\right| dt$. This procedure is repeated until $u^{(m)}(t)$ converges. This method

can also be used to obtain the DM soliton solutions of the PNLS equation and the solid line curves in Figure 10.9.

10.4.5 The higher-order DMNLS equation

The analysis of Section 10.4 can be taken to the next order in z_a (Ablowitz et al., 2002b). In the Fourier domain we write the more general DMNLS equation in the form

$$i\hat{U}_z - \frac{\langle d\rangle}{2}\omega^2\hat{U} + \overbrace{\int_{-\infty}^{\infty}\int_{-\infty}^{\infty} d\omega_1\, d\omega_2\, \hat{U}(\omega+\omega_1)\hat{U}(\omega+\omega_2)\hat{U}^*(\omega+\omega_1+\omega_2)r(\omega_1\omega_2)}^{n_0(\omega,z)} = z_a\hat{n}_1(\omega,z) + \cdots .$$

The method is similar to those described earlier for water waves and nonlinear optics. We find $\hat{n}_1$ such that the secular terms at higher order are removed. Recalling $u = u_0 + \epsilon u_1 + \epsilon^2 u_2 + \cdots$ where $\epsilon = z_a$, we substitute this into the perturbed NLSE equation (10.21), and as before employ multiple scales. We find

$$\begin{aligned} O\left(\epsilon^{-1}\right): &\quad \mathcal{L}u_0 = i\frac{\partial u_0}{\partial\zeta} + \frac{\Delta(z)}{2}\frac{\partial^2 u_0}{\partial t^2} = 0 \\ O(1): &\quad \mathcal{L}u_1 = -\left(i\frac{\partial u_0}{\partial Z} + \frac{\langle d\rangle}{2}\frac{\partial u_0}{\partial t^2} + g(\zeta)\left|u_0\right|^2 u_0\right) \\ O(\epsilon): &\quad \mathcal{L}u_2 = -\left(i\frac{\partial u_1}{\partial Z} + \frac{\langle d\rangle}{2}\frac{\partial u_1}{\partial t^2} + g(\zeta)\left(2\left|u_0\right|^2 u_1 + u_0^2 u_1^*\right)\right). \end{aligned}$$

The first two terms are the same as what we found earlier for the DMNLS equation. At $O\left(\epsilon^{-1}\right)$,

$$u_0 = \hat{U}(\omega, Z)e^{-i\omega^2 C(\zeta)/2}, \quad C(\zeta) = \int_0^{\zeta}\Delta(\zeta')\,d\zeta',$$

and at $O(1)$

$$\begin{aligned} i\frac{\partial\hat{u}_1}{\partial\zeta} - \frac{\Delta(\zeta)}{2}\omega^2\hat{u}_1 &= -\left(i\frac{\partial\hat{u}_0}{\partial Z} - \frac{\langle d\rangle}{2}\omega^2\hat{u}_0 + g(\zeta)\mathcal{F}\left\{\left|u_0\right|^2 u_0\right\}\right) \\ &= -\left(i\frac{\partial\hat{U}}{\partial Z} - \omega^2\frac{\langle d\rangle}{2}\hat{U}\right)e^{-i\omega^2 C(\zeta)/2} - g\mathcal{F}\left\{\left|u_0\right|^2 u_0\right\}. \end{aligned}$$

Thus,

$$\frac{\partial}{\partial\zeta}\left(i\hat{u}_1 e^{iC(\zeta)\omega^2/2}\right) = -\left(i\frac{\partial\hat{U}}{\partial Z} - \omega^2\frac{\langle d\rangle}{2}\hat{U}\right) - g(\zeta)e^{iC(\zeta)\omega^2/2}\mathcal{F}\left\{|u_0|^2 u_0\right\} \equiv \hat{F}_1.$$

To remove secular terms we enforce periodicity of the right-hand side, i.e., we require $\left\langle \hat{F}_1 \right\rangle = 0$, where $\left\langle \hat{F}_1 \right\rangle = \int_0^1 \hat{F}_1\, d\zeta$. This implies

$$i\frac{\partial\hat{U}}{\partial Z} - \omega^2\frac{\langle d\rangle}{2}\hat{U} + \hat{n}_0(\omega, Z) = 0,$$

with

$$\hat{n}_0(\omega, Z) = \left\langle g(\zeta)e^{i\omega^2 C(\zeta)/2}\mathcal{F}\left\{|u_0|^2 u_0\right\}\right\rangle.$$

This is the DMNLS equation (10.25) that can be transformed to (10.30).

We now take

$$i\frac{\partial\hat{U}}{\partial Z} - \omega^2\frac{\langle d\rangle}{2}\hat{U} + \hat{n}_0(\omega, Z) = \epsilon\hat{n}_1(\omega, Z) + \cdots. \tag{10.40}$$

Once we obtain $\hat{n}_1(\omega, Z)$ then (10.40) will be the higher-order DMNLS equation. However we need to solve for u_1 since it will enter into the calculation for n_1. Using an integrating factor in the $O(1)$ equation, adding and subtracting a mean term and using the DMNLS equation, we find

$$\begin{aligned}\frac{\partial}{\partial\zeta}\left(i\hat{u}_1 e^{iC(\zeta)\omega^2/2}\right) &= -\left[\left(i\frac{\partial U}{\partial Z} - \omega^2\frac{\langle d\rangle}{2}U\right) + \left\langle g(\zeta)e^{i\omega^2 C(\zeta)/2}\mathcal{F}\left\{|u_0|^2 u_0\right\}\right\rangle\right] \\ &\quad - g(\zeta)e^{i\omega^2 C(\zeta)/2}\mathcal{F}\left\{|u_0|^2 u_0\right\} + \left\langle g(\zeta)e^{i\omega^2 C(\zeta)/2}\mathcal{F}\left\{|u_0|^2 u_0\right\}\right\rangle \\ i\hat{u}_1 e^{iC(\zeta)\omega^2/2} &= -\int_0^\zeta g(\zeta)e^{i\omega^2 C(\zeta)/2}\mathcal{F}\left\{|u_0|^2 u_0\right\} d\zeta \\ &\quad + \zeta\left\langle g(\zeta)e^{i\omega^2 C(\zeta)/2}\mathcal{F}\left\{|u_0|^2 u_0\right\}\right\rangle + \hat{U}_{1H}(\omega, Z).\end{aligned}$$

Therefore,

$$\begin{aligned}\hat{u}_1 e^{iC(\zeta)\omega^2/2} =& i\int_0^\zeta g(\zeta)e^{i\omega^2 C(\zeta)/2}\mathcal{F}\left\{|u_0|^2 u_0\right\} d\zeta \\ &- i\zeta\left\langle g(\zeta)e^{i\omega^2 C(\zeta)/2}\mathcal{F}\left\{|u_0|^2 u_0\right\}\right\rangle - i\hat{U}_{1H}(\omega, Z),\end{aligned}$$

where $\hat{U}_{1H}(\omega, Z)$ is an integration "constant" to be determined. We choose $U_1(\omega, Z)$ such that $\left\langle u_1(\omega, Z) e^{iC(\zeta)\omega^2/2} \right\rangle = \int_0^1 u_1 e^{iC(\zeta)\omega^2/2}\, d\zeta = 0$. This is done to ensure that u_1 does not produce secular terms at next order. Therefore

$$\hat{U}_{1H} = \left\langle \int_0^\zeta g(\zeta') e^{i\omega^2 C(\zeta')/2} \mathcal{F}\left\{|u_0|^2 u_0\right\} d\zeta' \right\rangle - \frac{1}{2}\left\langle g(\zeta) e^{i\omega^2 C(\zeta)/2} \mathcal{F}\left\{|u_0|^2 u_0\right\}\right\rangle.$$

This fixes $\hat{u}_1$ and thus u_1. Then u_2 is given by

$$\frac{\partial}{\partial \zeta}\left(i\hat{u}_2 e^{iC(\zeta)\omega^2/2}\right) = -\left\{\hat{n}_1(\omega, Z) + e^{iC(\zeta)\omega^2/2}\left[i\frac{\partial \hat{u}_1}{\partial Z} - \right.\right.$$
$$\left.\left. - \frac{\langle d\rangle}{2}\omega^2 \hat{u}_1 + g(\zeta)\hat{P}_1(\zeta, Z, \omega)\right]\right\} \equiv \hat{F}_2,$$

where $\hat{P}_1 = \mathcal{F}\left\{2|u_0|^2 u_1 + u_0^2 u_1^*\right\}$. To eliminate secularities we require $\left\langle \hat{F}_2 \right\rangle = 0$. This condition determines $\hat{n}_1$ and we obtain the higher-order DMNLS equation. Thus, since $\left\langle \hat{u}_1 e^{iC(\zeta)\omega^2/2} \right\rangle = 0$, we have

$$\hat{n}_1 = -\left\langle g(\zeta) e^{i\omega^2 C(\zeta)/2} \hat{P}_1(\omega, Z)\right\rangle. \tag{10.41}$$

With $\hat{n}_0$ and $\hat{n}_1$ we now have the higher-order DMNLS equation (10.40). The form (10.41) is useful numerically. But as with the standard DMNLS theory we also note that we can write $\hat{n}_1$ as a multiple integral in the Fourier domain. After manipulation we find,

$$\hat{n}_1 = \frac{-i}{(2\pi)^4}\int_{-\infty}^{\infty}\int_{-\infty}^{\infty}\int_{-\infty}^{\infty}\int_{-\infty}^{\infty} d\omega_1\, d\omega_2\, d\Omega_1\, d\Omega_2\; r_1(\omega_1\omega_2, \Omega_1\Omega_2)$$
$$\left\{2\hat{U}(\omega+\omega_1)\times \hat{U}^*(\omega+\omega_1+\omega_2)\hat{U}(\omega+\omega_2+\Omega_1)\hat{U}(\omega+\omega_2+\Omega_2)\right.$$
$$\times \hat{U}^*(\omega+\omega_2+\Omega_1+\Omega_2) - \hat{U}(\omega+\omega_1)\hat{U}(\omega+\omega_2)\hat{U}^*(\omega+\omega_1+\omega_2+\Omega_1)$$
$$\left.\times\, \hat{U}(\omega+\omega_1+\omega_2-\Omega_2)\hat{U}(\omega+\omega_1+\omega_2+\Omega_1-\Omega_2)\right\}, \tag{10.42}$$

where the kernel is given by

$$r_1(x, y) = \left\langle g(\zeta)K(\zeta, x)\int_0^\zeta g(\zeta')K(\zeta', y)\, d\zeta' \right\rangle$$
$$- \langle g(\zeta)K(\zeta, x)\rangle \left\langle \int_0^\zeta g(\zeta')K(\zeta', y)\, d\zeta' \right\rangle$$
$$- \left\langle (\zeta - \tfrac{1}{2})g(\zeta)K(\zeta, x)\right\rangle \langle g(\zeta)K(\zeta, y)\rangle,$$

with $K(\zeta, z) = e^{iC(\zeta)z}$. When $g(\zeta) = 1$ (i.e., a lossless system), it is found that

$$r_1(x,y) = \frac{i(2\theta-1)}{2s^3(xy)^2(x+y)}\Big[sxy(y\cos sx\sin sy - x\cos sy\sin sx) + (x^2-y^2)\sin sx\sin sy\Big].$$

Note that when $g=1$, r_1 depends on s and θ separately, whereas when $g=1$ the kernel r in the DMNLS equation only depends on s (recall: $r(x) = \frac{sx}{(2\pi)^2 sx}$). The higher-order DMNLS (HO-DMNLS) equation (10.40) with the terms, $\hat{n}_0(\omega, Z)$, $\hat{n}_0(\omega, Z)$, derived in this section has a class of interesting solutions. With the HO-DMNLS, a wide variety of solutions including multi-hump soliton solutions can be obtained. Interestingly, single-humped, two-humped, three-humped, four-humped, etc., solutions are found. They also come with phases, for example, bi-solitons with positive and negative humps, as schematically illustrated in Figure 10.11. It has been conjectured that there exists an infinite family of such DMNLS solitons (Ablowitz et al., 2002b); see also Maruta et al. (2002).

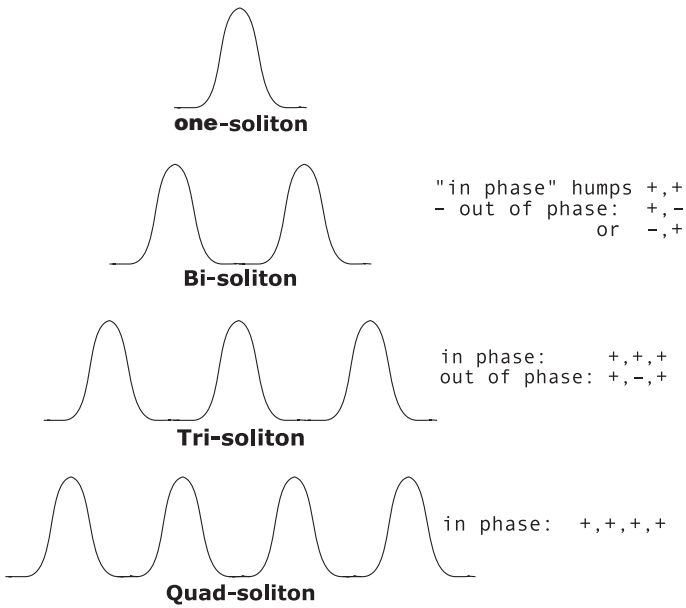

Figure 10.11 The HO-DMNLS equation has different families of soliton solutions, including the single soliton, also found in the DMNLS equation, and new multi-soliton solutions. Amplitude is plotted; + denotes a positive hump, whereas − denotes a negatives hump.

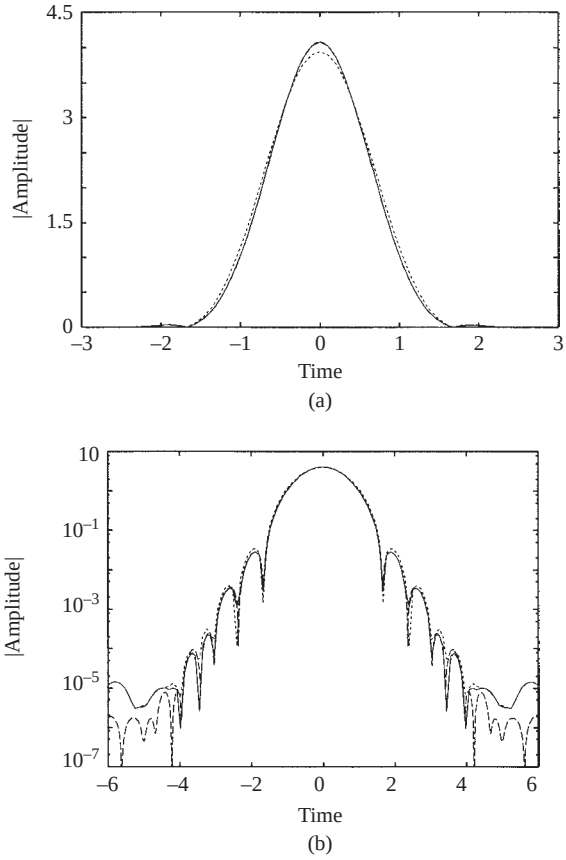

Figure 10.12 The solid curve is the approximate solution $u(t) = u_0(t) + z_a u_1(t)$, which is calculated from (10.40)–(10.42) with typical parameters and $g = 1$. The dashed curve represents a DM soliton obtained from the averaging method (see Section 10.4.4) on the PNLS equation (10.19) with $g = 1$; it is indistinguishable from the solid curve. The dotted curve is $U_0(t)$, which is the inverse Fourier transform of $\hat{U}_0(\omega)$, the leading-order solution of the HO-DMNLS. The waveforms are shown in (a) linear and (b) log scale. In (a) the dashed curve is indistinguishable from the solid curve. See also Ablowitz et al. (2002b).

Shown in Figures 10.12 and 10.13 are typical comparisons of the HO-DMNLS solutions and the DMNLS solutions (here: $z_a = 0.06$, $\langle d \rangle = 1.65$, $s = 0.54$, $\theta = 0.8$). These figures show the extra detail gained by including the higher-order terms. Figure 10.14 shows a bi-soliton solution of the HO-DMNLS, which cannot be found from the first-order DMNLS equation because the parameter values require both s and θ to be given separately. Note

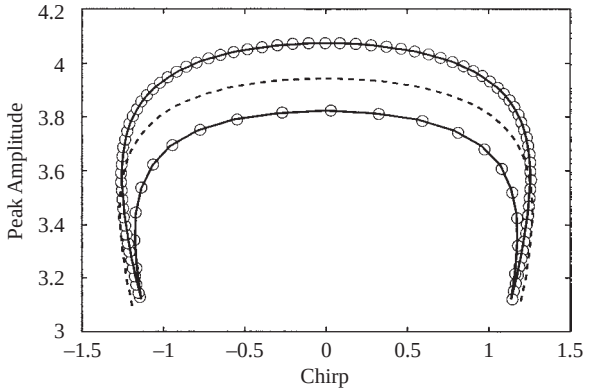

Figure 10.13 Evolution of chirp and peak amplitude of a DM soliton for typical parameters within a DM period. The solid curve and dashed curve denote the approximate solution $u(t) = u_0(t) + z_a u_1(t)$ and leading-order solution $u_0(t)$, respectively. The circles represent the evolution on the PNLS equation (10.19).

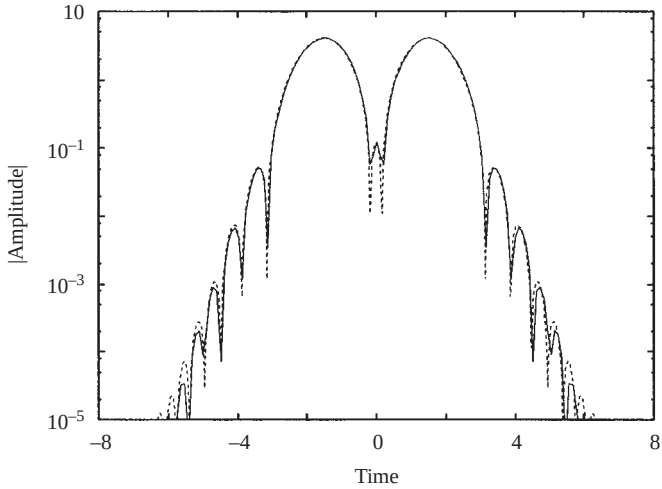

Figure 10.14 Bi-soliton solution with $\tau_s = 3t_{\mathrm{FWHM}}$, which is obtained by the averaging method (see Section 10.4.4) on the HO-DMNLS equation for $s = 0.56$, $\theta = 0.8$, $\langle d \rangle = 1.65$, and $M = 0.340$ (solid curve); recall $M = s/\langle d \rangle$ is the reduced map strength. The dotted curve shows the same solution that is given by the averaging method on the PNLS equation (here $g = 1$) (10.19).

that $M = s/\langle d \rangle$ is called the reduced map strength obtained by rescaling the HO-DMNLS equation (with $g = 1$) and finding that it can be rewritten by taking $\langle d \rangle = 1$ and replacing s by M in the HO-DMNLS equation (Ablowitz et al., 2002b).

10.5 Quasilinear transmission

A different type of pulse, termed "quasilinear", exists in strongly dispersion-managed transmission systems ($s \gg 1$) (Ablowitz et al., 2001b; Ablowitz and Hirooka, 2002). The analysis of this transmission mode begins with the DMNLS equation, discussed in Section 10.4.1,

$$i\hat{U}_Z - \frac{\langle d \rangle}{2}\omega^2 \hat{U} + \hat{N}\left[\hat{U}(\omega, Z)\right] = 0,$$

where

$$\hat{N}[\hat{U}(\omega, Z)] = \int_{-\infty}^{\infty}\int_{-\infty}^{\infty} d\omega_1\, d\omega_2\; \hat{U}(\omega+\omega_1) \times \hat{U}(\omega+\omega_2)\hat{U}^*(\omega+\omega_1+\omega_2) r(\omega_1\omega_2),$$

and

$$r(x) = \frac{1}{(2\pi)^2}\int_0^1 g(\zeta)\exp\left(-ixC(\zeta)\right)\, d\zeta.$$

Alternatively, as shown earlier, in the physical domain the DMNLS equation is given by

$$iU_z + \frac{\langle d \rangle}{2} U_{tt} + N[U] = 0,$$

where

$$N[U] = \int_{-\infty}^{\infty}\int_{-\infty}^{\infty} R(t_1, t_2) U(t+t_1) U(t+t_2) U^*(t+t_1+t_2)\, dt_1\, dt_2,$$

and

$$R(t_1, t_2) = \frac{1}{(2\pi)^2}\int_{-\infty}^{\infty}\int_{-\infty}^{\infty} r(\omega_1\omega_2) e^{i\omega_1 t_1 + \omega_2 t_2}\, d\omega_1\, d\omega_2.$$

In the lossless case we have seen in Section 10.4.2 that

$$\begin{aligned} R(t_1, t_2) &= \frac{1}{2\pi s}\mathrm{Ci}\left(\left|\frac{t_1 t_2}{s}\right|\right) \\ &= \frac{1}{2\pi s}\int_{\left|\frac{t_1 t_2}{s}\right|}^{\infty} \frac{\cos u}{u}\, du, \end{aligned}$$

where $Ci(x) \equiv \displaystyle\int_x^{\infty} \frac{\cos u}{u}\, du$ is the cosine integral.

In the quasilinear regime $s \gg 1$, so that in the asymptotic limit $s \to \infty$ we have $x = \left|\dfrac{t_1 t_2}{s}\right| \to 0$. We then use (see Section 10.5.1 below for further details),

$$\int_x^\infty \frac{\cos u}{u} du = -\gamma - \log x + O(x)$$

as $x \to 0$; γ is the so-called Euler constant. Thus,

$$R(t_1, t_2) \sim \frac{1}{2\pi s}\left(-\gamma - \log\left|\frac{t_1 t_2}{s}\right|\right) + O\left(s^{-1}\right),$$

and therefore

$$N(U) \sim \frac{1}{2\pi s}\int_{-\infty}^{\infty}\int_{-\infty}^{\infty}\left(-\gamma - \log\left|\frac{t_1 t_2}{s}\right|\right) U(t+t_1) \times U(t+t_2)U^*(t+t_1+t_2)\, dt_1\, dt_2.$$

Hence, taking the Fourier transform

$$\hat{N}\left[\hat{U}(\omega, Z)\right] \sim \frac{1}{2\pi s}\left\{(\log s - \gamma)|\hat{U}|^2\hat{U} - \mathcal{F}\left\{\log|t_1 t_2|\, U(t+t_1)U(t+t_2)U^*(t+t_1+t_2)\right\}\right\}.$$

With the Fourier transform of the last integral (see Section 10.5.1), we find

$$\mathcal{F}\left\{\log|t_1 t_2|\, U(t+t_1)U(t+t_2)U^*(t+t_1+t_2)\right\} = \frac{1}{\pi}\hat{U}(\omega)\int_{-\infty}^{\infty} dt\ \log|t|\, e^{i\omega t}\left[\int_{-\infty}^{\infty}|\hat{U}(\omega')|^2 e^{-i\omega' t}\, d\omega'\right].$$

Therefore

$$i\hat{U}_z - \frac{\langle d\rangle}{2}\omega^2\hat{U} + \Phi\left(|\hat{U}|^2\right)\hat{U} = 0, \tag{10.43}$$

where

$$\Phi\left(|\hat{U}|^2\right) = \frac{1}{2\pi s}\left[(\log s - \gamma)\left|\hat{U}(\omega)\right|^2 - \int_{-\infty}^{\infty} f(\omega-\omega')\left|\hat{U}(\omega')\right|^2\, d\omega'\right]$$

and $f(\omega) = \frac{1}{\pi}\int \log|t|\, e^{i\omega t} dt$. From (10.43) we find that $|\hat{U}(\omega, z)|^2 = |\hat{U}(\omega, 0)|^2 = |\hat{u_0}(\omega)|^2$. Therefore,

$$\hat{U}_z = -i\left[\frac{\langle d\rangle}{2}\omega^2 - \Phi\left(|\hat{U}_0|^2\right)\right]\hat{U},$$

and after integrating

$$\hat{U}(\omega, z) = \hat{U}(\omega, 0)\exp\left[-i\frac{\langle d\rangle}{2}\omega^2 z + i\Phi\left(|\hat{U}_0|^2\right)z\right]. \tag{10.44}$$

We refer to (10.44) as a quasilinear mode. When $g \neq 1$ the analysis is somewhat more complex and is derived in detail by Ablowitz and Hirooka (2002).

10.5.1 Analysis of the cosine integral and associated quasilinear Fourier integral

First we discuss an asymptotic limit of the cosine integral. Namely,

$$\mathrm{Ci}(x) = \int_x^\infty \frac{\cos t}{t}\, dt, \quad \text{as} \quad x \to 0+ .$$

Note that

$$\int_x^\infty \frac{\cos t}{t}\, dt = \mathrm{Re}\left\{ \int_x^\infty \frac{e^{it}}{t}\, dt \right\}.$$

where $\mathrm{Re}(x)$ represents the real part of x. Using the contour indicated in Figure 10.15 and appealing to Cauchy's theorem ($x > 0$),

$$\int_x^\infty \frac{e^{it}}{t}\, dt + \int_{C_R} \frac{e^{iz}}{z}\, dz + \int_{i\infty}^{ix} \frac{e^{iz}}{z}\, dz + \int_{C_\varepsilon} \frac{e^{iz}}{z}\, dz = 0.$$

Since $\mathrm{Im}\{z\} > 0$ on C_R, we have

$$\lim_{R\to\infty} \int_{C_R} \frac{e^{iz}}{z}\, dz = 0.$$

On the quarter circle at the origin, we get

$$\lim_{\epsilon\to 0} \int_{C_\epsilon} \frac{e^{iz}}{z}\, dz = \lim_{\epsilon\to 0} \int_{\pi/2}^{0} \frac{e^{i\epsilon e^{i\theta}}}{\epsilon e^{i\theta}} i\epsilon e^{i\theta}\, d\theta = -i\frac{\pi}{2}.$$

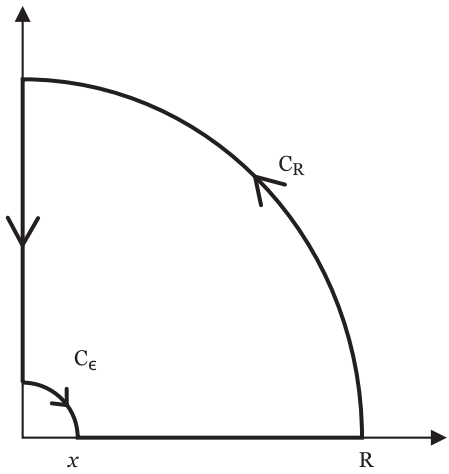

Figure 10.15 Integration contour.

Therefore we have

$$\int_x^\infty \frac{e^{it}}{t}\,dt = \int_{ix}^{i\infty} \frac{e^{iz}}{z}\,dz + i\frac{\pi}{2} = \int_x^\infty \frac{e^{-y}}{y}\,dy + i\frac{\pi}{2};$$

thus,

$$I \equiv \int_x^\infty \frac{\cos t}{t}\,dt = \Re\left\{\int_x^\infty \frac{e^{it}}{t}\,dt\right\} = \int_x^\infty \frac{e^{-y}}{y}\,dy.$$

Now,

$$I = \int_x^\infty \left(\frac{e^{-y}}{y} - \frac{1}{y(y+1)}\right)dy + \int_x^\infty \frac{1}{y(y+1)}\,dy$$
$$= \int_0^\infty \frac{\left(e^{-y} - \frac{1}{y+1}\right)}{y}\,dy + \int_0^x \frac{\left(e^{-y} - \frac{1}{y+1}\right)}{y}\,dy + \int_x^\infty \frac{1}{y(y+1)}\,dy.$$

Note that

$$\frac{e^{-y} - \frac{1}{y+1}}{y} \sim e^{-y} - (1 - y + y^2 - \cdots)$$
$$\sim \left[1 - y + \frac{y^2}{2} - \cdots - (1 - y + y^2 - \cdots)\right]/y$$
$$\sim -\frac{y}{2} + \cdots,$$

showing the integral $\int_0^\infty \frac{e^{-y} - \frac{1}{y+1}}{y}\,dy$ is convergent as $y \to 0$ (the integral clearly converges at the infinite upper limit) and it is well known that

$$\int_0^\infty \frac{\left(e^{-y} - \frac{1}{y+1}\right)}{y}\,dy \equiv -\gamma,$$

where γ is the Euler constant $\gamma \simeq 0.57722$. Also

$$\int_0^x \frac{\left(e^{-y} - \frac{1}{y+1}\right)}{y}\,dy \underset{x\to 0}{\sim} -\frac{x^2}{2} + \cdots$$

Similarly,

$$\int_x^\infty \frac{1}{y(y+1)}\,dy = \int_x^\infty \left(\frac{1}{y} - \frac{1}{y+1}\right)dy$$
$$= \log(1+x) - \log(x) \underset{x\to 0}{\sim} x - \log x.$$

Putting this all together implies, as $x \to 0+$,

$$I \sim -\gamma - \log x + x + O(x^2).$$

We now consider the Fourier integral

$$\begin{aligned}\mathrm{F} =& \mathcal{F}\left\{\int_{-\infty}^{\infty}\int_{-\infty}^{\infty}\log|t_1t_2|\,U(t+t_1)U(t+t_2)U^*(t+t_1+t_2)\,dt_1\,dt_2\right\}\\ =&\frac{1}{(2\pi)^3}\int_{-\infty}^{\infty}e^{-i\omega t}\,dt\iint dt_1\,dt_2\;\log|t_1t_2|\left[\int_{-\infty}^{\infty}\hat{U}(\omega_1)e^{i\omega_1(t+t_1)}\,d\omega_1\right]\\ &\times\left[\int_{-\infty}^{\infty}\hat{U}(\omega_2)e^{i\omega_2(t+t_2)}\,d\omega_2\right]\left[\int_{-\infty}^{\infty}\hat{U}^*(\omega_3)e^{-i\omega_3(t+t_1+t_2)}\,d\omega_3\right].\end{aligned}$$

Noting that the function is symmetric in t_1, t_2 and using $\int dt_2\; e^{i\omega_2t_2}e^{-i\omega_3t_2} = 2\pi\delta(\omega_2-\omega_3)$, we have

$$\begin{aligned}\mathrm{F} =&\frac{2}{(2\pi)^2}\int_{-\infty}^{\infty}dt\;\int_{-\infty}^{\infty}dt_1\;\log|t_1|\\ &\int_{-\infty}^{\infty}\int_{-\infty}^{\infty}\int_{-\infty}^{\infty}d\omega_1\,d\omega_2\,d\omega_3\;e^{i(\omega_1-\omega_3)t_1}\hat{U}(\omega_1)\hat{U}(\omega_2)\hat{U}^*(\omega_3)\\ &\times\delta(\omega_2-\omega_3)e^{i(\omega_1+\omega_2-\omega_3-\omega)t}\\ =&\frac{1}{2\pi^2}\int_{-\infty}^{\infty}dt\;\int_{-\infty}^{\infty}dt_1\;\log|t_1|\int_{-\infty}^{\infty}d\omega_1d\omega_3\;\hat{U}(\omega_1)\hat{U}(\omega_3)\hat{U}^*(\omega_3)\\ &\times e^{i(\omega_1-\omega)t}e^{i(\omega_1-\omega_3)t_1}.\end{aligned}$$

Using $\int_{-\infty}^{\infty}dt\;e^{i(\omega_1-\omega)t} = 2\pi\delta(\omega_1-\omega)$ implies

$$F=\frac{1}{\pi}\int_{-\infty}^{\infty}dt_1\;\log|t_1|\int_{-\infty}^{\infty}d\omega_3\;\hat{U}(\omega)\left|\hat{U}(\omega_3)\right|^2e^{i(\omega-\omega_3)t_1}.$$

Or finally,

$$\mathrm{F}=\hat{U}(\omega)\int_{-\infty}^{\infty}\left|\hat{U}(\omega')\right|^2f(\omega-\omega')\,d\omega',$$

where $f(x)$ is the generalized function,

$$f(x)=\int_{-\infty}^{\infty}dt\;\frac{\log|t|}{\pi}e^{ixt}.$$

For calculation, it is preferable to use F in the form

$$\mathrm{F}=\frac{1}{\pi}\hat{U}(\omega)\int_{-\infty}^{\infty}dt\;\log|t|\,e^{i\omega t}\left[\int_{-\infty}^{\infty}\left|\hat{U}(\omega')\right|^2e^{-i\omega' t}\,d\omega'\right].$$

When a Gaussian shape is taken, $|\hat{U}(\omega)| = \alpha e^{-\beta\omega^2}$, then the inner integral decays rapidly as $|t|\to\infty$.

10.6 WDM and soliton collisions

As mentioned earlier, in a WDM system solitons are transmitted at many different wavelengths, or frequencies; these different wavelengths are often called "channels". Due to the dispersion in the fiber, solitons at different wavelengths travel at different velocities. This leads to inevitable collisions between solitons in different wavelength channels.

Considering the case of only two WDM channels, centered at the normalized radial frequencies Ω_1 and Ω_2 we take two pulses u_1 and u_2 in channel 1 and 2 respectively. The average frequency of the pulses can be calculated as

$$\langle\omega\rangle = \mathrm{Im}\left\{\int_{-\infty}^{\infty} u_j^* \frac{\partial u_j}{\partial t}\, dt\right\} / W_j = \frac{1}{2\pi W_j}\int_{-\infty}^{\infty} \omega|\hat{u}_j(\omega)|^2\, d\omega, \tag{10.45}$$

where $\hat{u}_j(\omega)$ is the Fourier transform of $u(t)$, $W_j = \int_{-\infty}^{\infty} |u_j(t)|^2\, dt$, the energy of pulse u_j, and $j \in \{1, 2\}$ is the channel number. The right-hand side of (10.45) is obtained by replacing $u(t)$ by its Fourier transform.

In Section 10.2.1, we saw that the NLS equation with XPM contributions [see (10.12) and (10.13)] for channel 1 (u_1) is

$$i\frac{\partial u_1}{\partial z} + \frac{1}{2}\frac{\partial^2 u_1}{\partial t^2} + g(z)|u_1|^2 u_1 = -2g(z)|u_2|^2 u_1 \tag{10.46}$$

and for channel 2 (u_2) is

$$i\frac{\partial u_2}{\partial z} + \frac{1}{2}\frac{\partial^2 u_2}{\partial t^2} + g(z)|u_2|^2 u_2 = -2g(z)|u_1|^2 u_2.$$

We assume the signals u_1 and u_2 have negligible overlap in the frequency domain and that the FWM contribution is small. This assumption enables us to separate the components at different frequencies in the original perturbed NLS (PNLS) equation; i.e., one considers each equation as being valid in separate regions of Fourier space.

Assuming W_j is constant, the change in average frequency can be found from (10.45):

$$\begin{aligned} W_j \frac{d}{dz}\left\langle\omega_j\right\rangle &= \frac{\partial}{\partial z}\,\mathrm{Im}\left\{\int_{-\infty}^{\infty} \frac{\partial u_j}{\partial t} u_j^*\, dt\right\}, \\ &= \mathrm{Im}\left\{\int_{-\infty}^{\infty}\left(\frac{\partial^2 u_j}{\partial t \partial z} u_j^* + \frac{\partial u_j}{\partial t}\frac{\partial u_j^*}{\partial z}\right) dt\right\}. \end{aligned} \tag{10.47}$$

The NLS equation for channel u_1 with a perturbation F_1 is

$$iu_{1z} + \frac{d}{2}u_{1tt} + g|u_1|^2 u_1 = F_1.$$

Operating on the above equation with $-iu_1^*\partial_t$ and adding to the result iu_{1t} times the complex conjugate of the above equation, we find

$$\frac{\partial^2 u_j}{\partial t \partial z}u_j^* + \frac{\partial u_j}{\partial t}\frac{\partial u_j^*}{\partial z} = \frac{id}{2}\left(u_1^* u_{1ttt} - u_{1t}u_{1tt}^*\right) + ig\left(u_1^*\partial_t(|u_1|^2 u_1) - |u_1|^2 u_{1t}^*\right) + i\left(u_{1t}F_1^* - u_1^* F_{1t}\right).$$

Substituting this result into (10.47) and integrating the first two terms by parts (assuming u_1 and its derivatives vanish at $t = \pm\infty$), we find

$$W_1\frac{d\langle\omega_1\rangle}{dz} = \mathrm{Im}\left\{\int_{-\infty}^{\infty} i\left(F_1 u_{1t}^* + F_1^* u_{1t}\right)dt\right\} = \int_{-\infty}^{\infty}\left(F_1 u_{1t}^* + F_1^* u_{1t}\right)dt.$$

If we take $F_1 = -2g(z)|u_2|^2 u_1$ as indicated by (10.46), then

$$W_1\frac{d\langle\omega_1\rangle}{dz} = 2g(z)\int_{-\infty}^{\infty}|u_1|^2\partial_t|u_2|^2\,dt,$$

or more generally

$$\frac{d\left\langle\omega_j\right\rangle}{dz} = \frac{2g(z)}{W_j}\int_{-\infty}^{\infty}|u_j|^2\partial_t|u_{3-j}|^2\,dt,\ \ j = 1,2. \tag{10.48}$$

The frequency shift is found by integrating (10.48). Similarly, the timing shift may be found from the definition of the average position in time, $\left\langle t_j\right\rangle$, $j = 1, 2$:

$$W_j\left\langle t_j\right\rangle = \int_{-\infty}^{\infty} t\,|u_j|^2\,dt.$$

Thus, again assuming W_j is constant,

$$\begin{aligned}
W_1\frac{d}{dz}\langle t_1\rangle &= \frac{\partial}{\partial z}\left(\int_{-\infty}^{\infty} t\,|u_1|^2\,dt\right)\\
&= \int_{-\infty}^{\infty} t\left(u_1^*\frac{\partial u_1}{\partial z} + \frac{\partial u_1^*}{\partial z}u_1\right)dt\\
&= \int_{-\infty}^{\infty} t\left\{u_1^*\left[\frac{id}{2}u_{1tt} + ig(z)u_1^2 u_1^* - iF_1\right]\right\}dt\\
&\quad + \int_{-\infty}^{\infty} t\left\{u_1\left[-\frac{id}{2}u_{1tt}^* - ig(z)\left(u_1^*\right)^2 u_1 + iF_1^*\right]\right\}dt\\
&= -i\frac{d}{2}\int_{-\infty}^{\infty}\left(u_1^* u_{1t} - u_1 u_{1t}^*\right)dt - i\int_{-\infty}^{\infty} t\left(u_1^* F_1 - u_1 F_1^*\right)dt.
\end{aligned}$$

Recalling

$$W_j \left\langle \omega_j \right\rangle = \mathrm{Im}\left\{ \int_{-\infty}^{\infty} \frac{\partial u_j}{\partial t} u_j^* \, dt \right\} = \frac{1}{2i} \int_{-\infty}^{\infty} \left(\frac{\partial u_j}{\partial t} u_j^* - \frac{\partial u_j^*}{\partial t} u_j \right) dt,$$

we can write

$$W_1 \frac{d}{dz} \langle t_1 \rangle = d(z) W_1 \langle \omega_1 \rangle - i \int_{-\infty}^{\infty} t \left(u_1^* F_1 - u_1 F_1^* \right) \, dt.$$

Using $F_1 = -2g(z)|u_2|^2 u_1$, the integral $\int_{-\infty}^{\infty} t \left(u_1^* F_1 - u_1 F_1^* \right) dt = 0$ and we obtain

$$\frac{d}{dz} \langle t_1 \rangle = d(z) \langle \omega_1 \rangle . \tag{10.49}$$

The timing shift may be obtained by integrating (10.49) with respect to z.

In the context of RZ (return to zero) soliton or quasilinear communications systems it is useful to define the residual frequency shift as the relative frequency shift of the pulse at the end of the communications system. Using a system starting at $z = 0$ and of length L, with this definition the residual frequency shift of a pulse in channel j is given by

$$\Delta\Omega_{\mathrm{res}}^{(j)} = \left\langle \omega_j \right\rangle (L) - \langle \omega \rangle (0) = \int_0^L \frac{d \left\langle \omega_j \right\rangle}{dz} \, dz.$$

We are also interested in the relative timing shift at the end of the collision process. The total timing shift, (10.49), yields

$$\begin{aligned} \frac{d}{dz} \left\langle t_j \right\rangle (z) &= d(z) \left[\left\langle \omega_j \right\rangle (z) - \left\langle \omega_j \right\rangle (0) \right] + d(z) \left\langle \omega_j \right\rangle (0) \\ &= d(z) \int_0^z \frac{d \left\langle \omega_j \right\rangle}{dz} \, dz + d(z) \left\langle \omega_j \right\rangle (0). \end{aligned}$$

Defining $\bar{d}(z) = \int_0^z d(z') \, dz'$, and integrating the above equation from $z = 0$ to $z = L$,

$$\left\langle t_j \right\rangle (L) - \left\langle t_j \right\rangle (0) = \int_0^L d(z) \int_0^z \frac{d \langle \omega \rangle_j}{dz'} \, dz' \, dz + \bar{d}(L) \left\langle \omega_j \right\rangle (0).$$

Note that $\left\langle t_j \right\rangle (0) + \bar{d}(L) \left\langle \omega_j \right\rangle (0)$ is invariant. We can also define the relative timing shift as

$$\Delta t_j(L) \equiv \left\langle t_j \right\rangle (L) - \left\langle t_j \right\rangle (0) - \bar{d}(L) \left\langle \omega_j \right\rangle (0) = \int_0^L d(z) \int_0^z \frac{d \langle \omega \rangle_j}{dz'} \, dz' \, dz.$$

This can now be simplified by changing the order of integration:

$$\begin{aligned}\Delta t_j(L) &= \int_0^L d(z) \int_0^z \frac{d\,\langle\omega\rangle_j}{dz'}\,dz'\,dz \\ &= \int_0^L \frac{d\,\langle\omega\rangle_j}{dz'} \int_{z'}^L D(z)\,dz\,dz' \\ &= \int_0^L \frac{d\,\langle\omega\rangle_j}{dz'} \left[\bar{d}(L) - \bar{d}(z')\right] dz' \\ &= \bar{d}(L) \int_0^L \frac{d\,\langle\omega\rangle_j}{dz'}\,dz' - \int_0^L \frac{d\,\langle\omega\rangle_j}{dz'} \bar{d}(z')\,dz' \\ &= \bar{d}(L)\Delta\Omega_{\rm res}^{(j)} - \int_0^L \frac{d\,\langle\omega\rangle_j}{dz'} \bar{d}(z')\,dz'.\end{aligned} \tag{10.50}$$

Thus, the relative timing shift can be written as the difference of two terms:

$$\Delta t_j(L) = \bar{d}(L)\Delta\Omega_{\rm res}^{(j)} - \Delta t_{\rm res}^{(j)},$$

where the so-called residual timing shift is

$$\Delta t_{\rm res}^{(j)} \equiv \int_0^L \frac{d\,\langle\omega\rangle_j}{dz} \bar{d}(z)\,dz.$$

10.7 Classical soliton frequency and timing shifts

In this section we obtain the frequency and time shift for classical solitons; see also Mollenauer et al. (1991). Using the classical soliton shape

$$u_j = \eta_j\ \mathrm{sech}[\eta_j(t - \Omega_j z)]\ e^{i\Omega_j t + i\left(\eta_j^2 - \Omega^2\right)/2 + i\phi_j},$$

we substitute this into (10.48) to find

$$\begin{aligned}\frac{d\left\langle\omega_j\right\rangle}{dz} = \frac{g(z)}{\eta_j} \int_{-\infty}^{\infty} \frac{d}{dt} \left\{\eta_{3-j}^2\ \mathrm{sech}^2\left[\eta_{3-j}\left(t - \Omega_{3-j}(z - z_0)\right)\right]\right\} \\ \times \eta_j^2\ \mathrm{sech}^2\left[\eta_j\left(t - \Omega_j(z - z_0)\right)\right] dt.\end{aligned}$$

Note that the classical soliton frequency is $\left\langle\omega_j\right\rangle = \Omega_j$. For $|\Omega_j| \gg 1$ we take Ω_j approximately being a constant within the integral. Then we can transform the derivative in t to one in z:

$$\begin{aligned}\frac{d\Omega_j}{dz} = \frac{g(z)\eta_{3-j}^2\eta_j}{\Omega_{3-j}} \int_{-\infty}^{\infty} \frac{d}{dz} \left\{\mathrm{sech}^2\left[\eta_{3-j}\right.\right. \\ \left.\left. \times \left(t - \Omega_{3-j}(z - z_0)\right)\right]\right\}\ \mathrm{sech}^2\left[\eta_j\left(t - \Omega_j(z - z_0)\right)\right] dt.\end{aligned}$$

To simplify this integral we assume that the solitons are both of equal energy (amplitude) with $\eta_1 = \eta_2 = \eta$ and we take a frame of reference where $\Omega_1 = -\Omega_2 = \Omega$. For an arbitrary frame of reference we may define Ω, without loss of generality, as half the frequency separation:

$$\Omega \equiv \frac{1}{2}(\Omega_1 - \Omega_2).$$

With this substitution the average frequency change can be simplified to

$$\frac{d\Omega}{dz} = \frac{g(z)\eta^3}{2\Omega}\frac{d}{dz}\int_{-\infty}^{\infty} \operatorname{sech}^2\left[\eta\left(t - \Omega(z - z_0)\right)\right] \times \operatorname{sech}^2\left[\eta\left(t + \Omega(z - z_0)\right)\right] dt.$$

Performing the integration in time analytically, we obtain an expression for the frequency shift, $\Delta\Omega = \Omega(z) - \Omega(-\infty)$ (we take the "initial" frequency to be given at large negative values of z that is taken to be $-\infty$):

$$\Delta\Omega(z) = \frac{2\eta^2}{\Omega} \times \int_{-\infty}^{z} g(z')\frac{d}{dz'}\frac{2\eta\Omega(z' - z_0)\cosh 2\eta\Omega(z' - z_0) - \sinh 2\eta\Omega(z' - z_0)}{\sinh^3 2\eta\Omega(z' - z_0)}\, dz'.$$

We can similarly calculate the timing shift. First we assume a constant dispersion of $d(z) = 1$. Then we can calculate the residual timing shift by using (10.50) (and integration by parts)

$$\Delta t(z) = \int_{-\infty}^{z} \Delta\Omega(z')\, dz'.$$

From these equations we can calculate the frequency and timing shifts for a classical soliton collision. A typical collision is shown in Figure 10.16, where the propagating path is shown explicitly; the soliton is injected into the system at $z = 0$ at a time position of t_0 for u_1 and $-t_0$ for u_2; they meet and collide with a collision center of z_0 and propagate onward until the end of the system at $z = L$. The initial location of the solitons, t_0, is related to the center of collision by

$$t_0 = \Omega D z_0.$$

The frequency shift is shown in Figure 10.17a over the distance of the collision relative to its center, z_0. The frequency shift is maximal at the center of the collision and returns to zero after the collision for the lossless case ($g = 1$). For the "lossy" case, $g \neq 1$ (i.e., with damping and amplification included

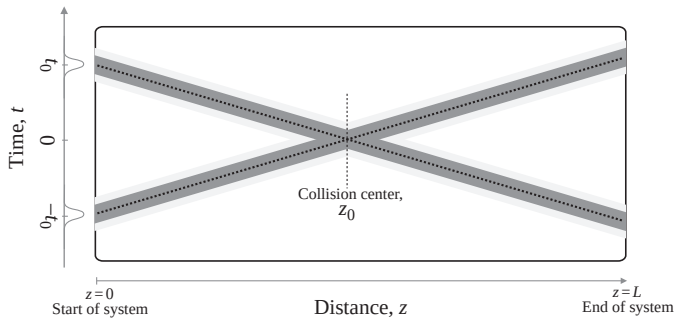

Figure 10.16 Two classical solitons colliding at z_0; the solitons have an equal but opposite velocity. The inset to the left shows the initial pulse envelope with solitons centered at t_0 and $-t_0$.

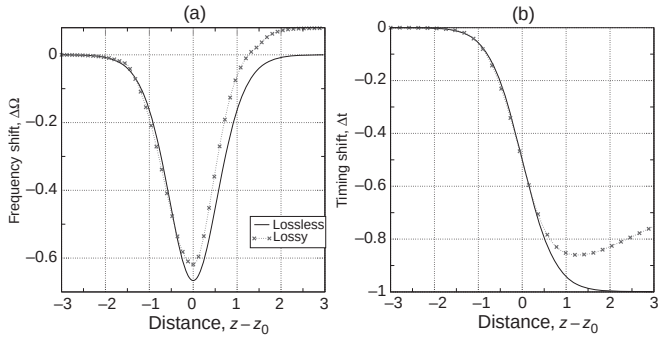

Figure 10.17 Typical frequency, (a), and timing, (b), shifts versus the distance over the collision $z - z_0$, with the collision center being at z_0 shown for both the lossless and lossy cases. Here $\Omega = 1$, ($g = 1$) for the lossless case and ($g \neq 1$) for the lossy case.

with the term $g(z)$) there is a considerable frequency shift after the collision process is complete. This is the residual frequency shift that in the total timing shift grows with z, see (10.50). This is especially damaging to classical soliton transmission.

The timing shifts for the same collisions are shown in Figure 10.17. Here it can be seen that after a collision the timing shift does not return to zero. When there is a residual frequency shift the timing shift continues to change after the collision. The total timing shift at the end of the communications channel is a combination of a fixed residual timing shift and a growing shift from the residual frequency shift; see (10.50).

10.8 Characteristics of DM soliton collisions

Collisions also occur in DM soliton systems. Solitons in different wavelength channels have a different *average* velocity and can therefore overlap and collide. Dispersion-management is characterized by rapidly varying large opposing dispersions that give the DM soliton (or any pulse in a DM system) large local velocities. This results in the "zig-zag" path characteristic of DM systems, as illustrated in Figure 10.18. These diversions from the average path become more pronounced as the DM map strength is increased and make DM soliton collisions quite different from collisions in a classical soliton system.

When two DM solitons collide they go through a collision process consisting of many individual "mini-collisions", where the solitons will meet and pass through each other completely in one half of the map only to change velocity and pass through each other on the next half, performing two mini-collisions per map period.

The collision center is defined as the center of the average paths of the solitons. For classical solitons changing z_0 changed the position of the collision in the system but did not change the outcome of the collision. In a DM system changing z_0 not only changes the position of the collision process, it also changes the position of the mini-collisions within the DM map. This in turn changes the nature of the collision process, and consequently the final frequency and timing shifts are dependent on z_0.

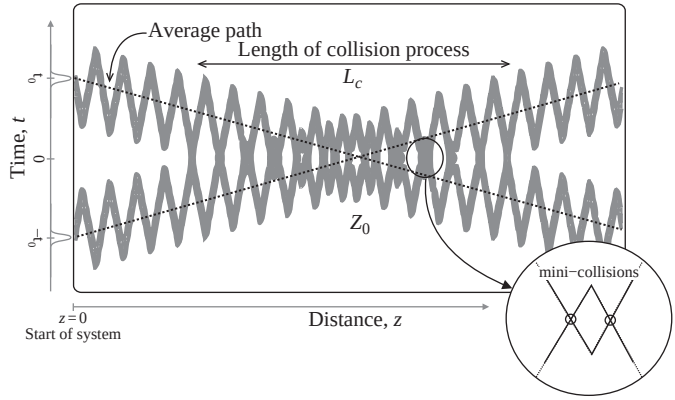

Figure 10.18 The movements of two colliding DM solitons, with an enlarged view of the soliton centers over a single DM map period, showing the intersections that are the mini-collisions.

As with classical soliton collisions the initial time displacement at the start of the channel can be calculated from the collision center, defined as

$$t_0 = \Omega_j \langle d \rangle z_0,$$

with $j \in \{1, 2\}$ indicating one of the two frequency channels.

The center of a DM soliton satisfies $t_c^{(n)} - \Omega_j \bar{d}(z) = 0$ for $t_c^{(n)}$ and z, with $n \in \{1, 2\}$ indicating one of the two frequency channels. An approximate analytical formula for a DM soliton is given in the next section; see (10.51). Using this we can find the locations of the mini-collisions, those values of z at which the centers of both solitons are coincident, namely $t_c^{(1)} = t_c^{(2)}$:

$$\Omega_1 \bar{d}(z) = \Omega_2 \bar{d}(z)$$

so that

$$\bar{d}(z) = 0.$$

Therefore mini-collision locations are found from the solution of $\bar{d}(z) = \langle d \rangle (z - z0) + C(z) = 0$, and are not influenced by the average frequencies of either soliton. The range of the chirp, $C(z)$, is limited; it periodically oscillates between $\min\{C(z)\}$ and $\max\{C(z)\}$. As a consequence $\bar{d}(z) = 0$ only has solutions over a limited domain, which corresponds to the extent of the collision process. When $\langle d \rangle (z - z_0)$ is larger or smaller than the range of $C(z)$, there are no mini-collisions, and we can therefore estimate the extent of the collision as

$$-\max\{C(z)\} < \langle d \rangle (z - z_0) < -\min\{C(z)\}$$
$$z_0 - s/\langle d \rangle < z < z_0 + s/\langle d \rangle,$$

where $\max\{C(z)\} = -\min\{C(z)\} = s = \theta\Delta_1/2$. The length of the collision $L_C = 2s/\langle d \rangle$ is the difference of the upper and lower collision limits, and we notice that the larger the map strength the longer is the DM soliton's collision process.

10.9 DM soliton frequency and timing shifts

We have seen in Section 10.4 that $\hat{u} = \hat{U}e^{-iC\omega^2/2}$. If we approximate $\hat{U}$ by $\hat{U} = \alpha e^{-\beta\omega^2/2}$, then a DM soliton can be approximated in physical space by

$$u_1(z, t) = \frac{\alpha}{\sqrt{2\pi(\beta + iC(z))}} \exp\left\{-\frac{[t - \Omega_1 \bar{d}(z)]^2}{2[\beta + iC(z)]}\right\} \times \exp\left\{\frac{i}{2}\left[\lambda^2 z + 2\Omega_1 t - \Omega_1^2 \bar{d}(z)\right]\right\}, \quad (10.51)$$

where $\bar{d}(z) - \langle d\rangle z_0 = \int_{z_0}^{z} d(z')\,dz' = (z - z_0)\langle d\rangle + C(z)$. Substituting the above DM soliton representation for u_1 and u_2 into (10.48) we get

$$\frac{d\left\langle\omega_j\right\rangle}{dz} = -\frac{g(z)\alpha_j\alpha_{3-j}\beta_{3-j}}{2\pi\left[\beta_j^2 + C^2(z)\right]^{1/2}\left[\beta_{3-j}^2 + C^2(z)\right]^{5/2}} \times \int_{-\infty}^{\infty}[t - \Omega_{3-j}\bar{d}(z)]\exp\left\{-\frac{\beta_j[t-\Omega_j\bar{d}(z)]^2}{2\left[\beta_j^2 + C^2(z)\right]} - \frac{\beta_{3-j}[t-\Omega_{3-j}\bar{d}(z)]^2}{2\left[\beta_{3-j}^2 + C^2(z)\right]}\right\} dt$$

for $j = 1, 2$. We further assume that the solitons in both channels have the same shape; that is, $\alpha_1 = \alpha_2$ and $\beta_1 = \beta_2$. With this assumption and noting $\left\langle\omega_j\right\rangle = \Omega_j$, we obtain an analytic formula for DM soliton collision-induced frequency shifts,

$$\frac{d\Omega_1}{dz} = (A/2)(\Omega_1 - \Omega_2)\frac{\bar{d}(z)g(z)}{B^3(z)}\exp\left(-(\beta/2)\left[\frac{\bar{d}(z)}{B(z)}(\Omega_1 - \Omega_2)\right]^2\right), \quad (10.52)$$

where $d\Omega_1/dz = -d\Omega_2/dz$ and in order to simplify this and equations that follow, we use the following definitions:

$$A = \frac{4W\beta^{3/2}}{\sqrt{2\pi}},$$
$$B^2(z) = \beta^2 + C^2(z/z_a).$$

We remark that in the case of quasilinear pulses the only difference turns out to be the definition of $B(z)$; for quasilinear pulses, we use $B^2(z) = \beta^2 + (\bar{d})^2(z)$. Because the two-channel system is symmetric, we can, without loss of generality, define $\Omega = (\Omega_1 - \Omega_2)/2$. The residual frequency shift, $\Delta\Omega(z) = \Omega(z) - \Omega(-\infty)$, is obtained by integration of (10.52). Assuming $\Omega(z)$ is a slowly varying function (i.e., $|d\Omega/dz| \ll 1$) which must be the case for the validity of the perturbation method (and is verified *a posteriori*), we can treat Ω on the right-hand side of (10.52) as a constant, obtaining

$$\Delta\Omega(z) = A\Omega\int_0^z \frac{g(z)\bar{d}(z)}{B^3(z)}\exp\left[-2\beta\left(\frac{\bar{d}(z)}{B(z)}\Omega\right)^2\right]dz. \quad (10.53)$$

We can also obtain the timing shift from (10.50):

$$\Delta t(L) = \bar{d}(L)\Delta\Omega(L) - \int_0^L \frac{d\langle\omega\rangle}{dz'}\bar{d}(z')\,dz'. \quad (10.54)$$

Ablowitz et al. (2002a, 2003b), Docherty (2003), and Ahrens (2006) the details of various types of collisions describe. There it is shown that direct numerical computation of the NLS equation agrees with numerical evaluation of (10.53) and (10.54), which also agree with asymptotic evaluation of (10.53) and (10.54) by employing the asymptotic analysis of integrals using a modification of the Laplace method.